Published in final edited form as:
Acta Neuropathol. 2012 June ; 123(6): 787–805. doi:10.1007/s00401-012-0987-3.

Cognitive defects are reversible in inducible mice expressing pro-aggregant full-length human Tau

Ann Van der Jeugd[#2], **Katja Hochgräfe**[#1,4], **Tariq Ahmed**[#2], **Jochen M. Decker**[#1], **Astrid Sydow**[3,4], **Anne Hofmann**[3,4], **Dan Wu**[1,3], **Lars Messing**[1], **Detlef Balschun**[2], **Rudi D'Hooge**[2], and **Eva-Maria Mandelkow**[1,3,§]

[(1)]DZNE (German Center for Neurodegenerative Diseases) and CAESAR Research Center, Ludwig-Erhard-Allee 2, 53175 Bonn, Germany

[(2)]Laboratory of Biological Psychology, Dept. Psychology, K.U.Leuven, Tiensestraat 102, 3000 Leuven, Belgium

[(3)]Max-Planck-Institute for Neurological Research, Gleuelerstr. 50, 50931 Cologne, Germany

[#] These authors contributed equally to this work.

Abstract

Neurofibrillary lesions of abnormal Tau are hallmarks of Alzheimer´s disease and frontotemporal dementias. Our regulatable (Tet-OFF) mouse models of tauopathy express variants of human full-length Tau in the forebrain (CaMKIIα promoter) either with mutation ΔK280 (pro-aggregant) or ΔK280/I277P/I308P (anti-aggregant). Co-expression of luciferase enables *in vivo* quantification of gene expression by bioluminescence imaging. Pro-aggregant mice develop synapse loss and Tau pathology including missorting, phosphorylation and early pretangle formation, whereas anti-aggregant mice do not. We correlated hippocampal Tau pathology with learning/memory performance and synaptic plasticity. Pro-aggregant mice at 16 months of gene expression exhibited severe cognitive deficits in Morris water-maze and in passive-avoidance paradigms, whereas anti-aggregant mice were comparable to controls. Cognitive impairment of pro-aggregant mice was accompanied by loss of hippocampal LTP in CA1 and CA3 areas and by a reduction of synaptic proteins and dendritic spines, although no neuronal loss was observed. Remarkably, memory and LTP recovered when pro-aggregant Tau was switched-OFF for ~4 months, Tau phosphorylation and missorting were reversed, and synapses recovered. Moreover soluble and insoluble pro-aggregant hTau40 disappeared while insoluble mouse Tau was still present. This study links early Tau pathology without neurofibrillary tangles and neuronal death to cognitive decline and synaptic dysfunction. It demonstrates that Tau-induced impairments are reversible after switching-OFF pro-aggregant Tau. Therefore our mouse model may mimic an early phase of AD when the hippocampus does not yet suffer from irreversible cell death but cognitive deficits are already striking. It offers potential to evaluate drugs with regard to learning and memory performance.

[§]**corresponding author:** Eva-Maria Mandelkow, Tel.: +49 228 43302-630, FAX: +49 228 43302-689, mandelkow@dzne.de.
[(4)]Current address: Max-Planck-Unit for Structural Molecular Biology, c/o Desy, Notkestr. 85, 22607 Hamburg, Germany

Conflict of interest
The authors declare that they have no conflict of interest.

Europe PMC Funders Author Manuscripts

Keywords

Alzheimer´s disease; Tau mouse model; behavior; long term potentiation; bioluminescene imaging

Introduction

Alzheimer´s disease (AD) is characterized clinically by a progressive cognitive decline with learning and memory impairment. Neurodegeneration, loss of synapses, neurons and the accumulation of insoluble protein aggregates are prominent neuropathological features of AD. Extracellular amyloid plaques mainly consist of aggregated Aβ peptide while intracellular neurofibrillary tangles (NFT) are composed of an abnormal form of the microtubule (MT)-associated Tau protein [65].

Tau is a highly soluble protein located mainly in axons, where it plays an important role in MT dynamics and axonal transport processes [43,44]. In pathological conditions Tau gets phosphorylated, mislocalizes to neuronal cell bodies and dendrites [28,74,80] and aggregates into NFTs [3]. Successful approaches to generate mouse models with AD-like Tau pathology include the introduction of Tau mutations, which cause frontotemporal dementias (FTD) [41,46] as well as combining Tau expression with enhanced Aβ activity [55]. In addition the usage of forebrain-specific promoters [e.g. calcium/calmodulin-dependent protein kinase II (CaMKIIα)] [45] restricted Tau expression to AD-relevant brain regions, thereby avoiding unwanted motor side effects caused by Tau expression in the spinal cord [33]. For some of these models functional impairments such as learning and memory deficits and electrophysiological dysfunctions have been described [6,37,62–64,72,79].

The AD mouse models used here carry the Tau mutation ΔK280 observed in FTDP-17 [76] in an inducible fashion (Tet-OFF). The mutation ΔK280 strongly increases Tau aggregation by enhancing the propensity of Tau to form β-structures (pro-aggregant Tau) [77]. In contrast the introduction of two additional proline mutations in the hexapeptide motifs (I277P and I308P) prevents Tau aggregation by disrupting the β-structure (anti-aggregant Tau) [34].

It turned out that AD-like pathology such as missorting, Tau phosphorylation, synapse loss and aggregation developed only in the presence of pro-aggregant Tau, regardless whether pro-aggregant full-length human Tau (hTau40, 2N4R) or the truncated “four-repeat” domain of Tau (Tau_{RD}) was expressed. No such deficits were observed expressing anti-aggregant variants of Tau [19,47]. In comparison to hTau40, truncated Tau_{RD} binds only weakly to MTs [22,27] and induces stronger neuropathological changes in terms of aggregation and neuronal loss, which are accompanied by memory and learning impairments and defects in neuroplasticity. Remarkably, this phenotype is reversible by switching-OFF the toxic Tau_{RD} mutant [69].

In this study we wanted to clarify whether the full-length variant hTau40-ΔK280 is capable of inducing functional deficits such as cognitive and synaptic impairments, even though it has a much lower β-propensity and neurotoxicity than the repeat domain Tau_{RD}-ΔK280. We addressed several issues: (1) Can pathological changes induced by exogenous pro-aggregant

Europe PMC Funders Author Manuscripts

hTau40 be correlated to cognitive impairments or defects in synaptic plasticity? (2) Are functional deficits based on overexpression or rather on aggregation of Tau? (3) Do cognitive and synaptic impairments recover after switching-OFF exogenous Tau expression? To answer these questions, we compared learning, memory, LTP and histopathology of mice where expression of pro and anti-aggregant human Tau was switched-ON to mice where expression of human Tau was first switched-ON and then OFF again. We found that expression of pro-aggregant full-length Tau leads to synaptic and cognitive defects, which are reversed after switch-OFF. Functional defects develop in the absence of neuronal loss and tangle formation, reconstructing an early phase of AD.

Material and Methods

Generation of pro- and anti-aggregant hTau40 transgenic mice

Transgenic mice expressing either pro- or anti-aggregant human full-length Tau were generated as described [19]. Non-transgenic littermates were used as controls. For switch-OFF experiments mice received doxycycline-containing food pellets (200mg/kg) for 0.5, 1, 2 or 4 months. All animal procedures were approved by the German Animal Welfare Act.

In vivo bioluminescence imaging of luciferase activity

In vivo bioluminescence imaging (BLI) was performed using an Ivis Spectrum imaging system (Caliper Life Science). Fifteen minutes prior to BLI, mice received an intraperitoneal injection of 150mg/kg D-luciferin (Caliper Life Science). Images were analyzed using Living Image 4.0 software (Caliper Life Science). The bioluminescence emission was normalized and the surface radiance was displayed in photons per second per centimeter squared per steradian (photons/s/cm^2/sr). For quantification of bioluminescence signals, a region of interest (ROI) was defined to convert surface radiance (photons/s/cm^2/sr) into total flux of the bioluminescent source (photons/s).

Preparation of brain homogenates and extraction of sarcosyl-insoluble Tau

Total Tau brain homogenates to detect synaptic proteins and sarcosyl-soluble and -insoluble fractions of Tau were isolated from brain tissue as described [26,69].

Immunoblot analysis

Western blots were carried out as described [69]. 2-5μg of total protein was loaded for the detection with pan-Tau antibody K9JA (1:20000, Dako), the human Tau specific antibody TauY9 (1:2000, Biosource), phospho-Tau antibodies 12E8 (pSer262/pSer356, 1:500, Elan), PHF-1 (pSer396/pSer404, 1:500, Dr. P. Davies), AT180 (pThr231/pSer235, 1:500, Pierce) and AT8 (pSer202/pThr205, 1:500, Thermo Scientific) and antibodies against synaptic proteins: synaptophysin (1:20000, Sigma), PSD95 (1:2000, Dianova) and GluR1 (1:1000, Millipore). Blots were normalized by the concentration of actin (1:20000, Sigma), developed using the ECL Plus detection system (GE Healthcare) and analyzed by densitometry (LAS 3000, AIDA software, Raytest).

Europe PMC Funders Author Manuscripts

Histology

Immunohistochemistry was performed on 5μm paraffin sections as described [69] using antibodies: TauY9 (1:1000, Biosource), 12E8 (1:500, Elan), MC-1 (1:10) and PHF-1 (1:50, both gifts from Dr. P. Davies, Albert Einstein College, NY), AT180 (1:1000, Pierce), NeuN (1:1000, Millipore). Fluorescent stainings were done on cryo sections of acute horizontal hippocampal slices using anti-synaptophysin (1:200, Sigma) and goat-anti mouse-Cy2 (Jackson Immunoresearch). Photomicrographs were taken with constant laser intensity. Mean pixel intensities/ROI were measured using ImageJ (NIH) and compared by students T-test (n = 3 mice/group).

Golgi staining and quantification of spines

For Golgi-Cox impregnations of neurons [21] the FD rapid GolgiStain™kit (FD NeuroTechnologies) was used according to the manufacturer´s protocol. Golgi-impregnated pyramidal neurons of the CA1 layer of the hippocampus were used for quantification of dendritic spines as described [59]. For each mouse (n = 3 per group) 10-13 neurons and 1-2 dendrites per neuron of 20-30μm lengths were quantified using ImageJ software (NIH) and were analyzed using Graph Pad Prism 5.0 software (Graph Pad). One-way analysis of variances (ANOVA) followed by Bonferroni´s post-hoc. Bars represent mean ± SEM.

Behavioral and memory tasks

Neuromotor tests—Grip strength, rotarod and cage activity was measured as described [69].

Morris water maze—Spatial memory abilities were examined in the standard hidden-platform acquisition and retention version of the Morris water maze [50]. Acquisition and probe trials were conducted as described [14,69]. Statistical comparison between groups and control littermates were accomplished by two-way repeated ANOVA (one factor repetition) followed by all pairwise multiple comparison procedures (Fisher LSD method). For analysis of probe trials one way ANOVA was performed.

Step-through passive avoidance task—Single-trial passive avoidance learning was examined in a step-through box with a small illuminated compartment and a larger dark compartment with a grid-floor as described [69]. The entry latency was recorded with a cut-off of 300s. For statistics one way ANOVA followed by all pairwise multiple comparison procedures (Fisher LSD method) was performed.

Electrophysiology

CA1 Schaffer collateral recordings—Preparation of hippocampal slices, extracellular electrophysiological recordings and analysis were carried out as described [69]. CA1 recordings of pro- and anti-aggregant mice were performed subsequently after finishing behavioral tests at the age of 16 months (16 months ON or 12 months ON + 4 months OFF).

CA3 mossy fiber recordings

Slice preparation: Horizontal hippocampal slices (400μm) were prepared from 12 months old mice (12 months ON or 8 months ON + 4 months OFF). To obtain optimal mossy fiber preservation a cutting-angle of 12° in the fronto-occipital direction was used [4]. Slices were transferred into an interface chamber and superfused with carbogenated ACSF (126mM NaCl, 21mM $NaHCO_3$, 3mM KCl, 2mM $CaCl_2$, 1.8mM $MgSO_4$, 1.25mM NaH_2PO_4 and 10mM glucose, saturated with 95% O_2/5% CO_2) at 36 ± 0.5°C; flow rate, 1.8ml/min; pH 7.4.

Recordings: After 1.5h, slices were transferred to a submerged recording chamber at 30°C. Extracellular field potentials (fEPSP) were recorded from *stratum lucidum* in area CA3. As stimulation electrode a patch-clamp pipette was used (1.5-2MΩ) to excite *mossy fibers* (mf) in the region of the *hilus*. Electrodes (2.5MΩ) were filled with ACSF and separated constantly 200μm from each other. fEPSPs were filtered at 1kHz, sampled at 10kHz and 10x preamplified (custom made preamplifier) using a HEKA double patch-clamp EPC 10 USB amplifier (HEKA Elektronik Dr. Schulze GmbH).

Stimulation protocols: Constant current pulses were elicited every 20s (0.05Hz) with a pulse width of 0.1ms. Input output (I/O) curves were generated using stimulus intensities ranging from 10-100μA with an increment of 10μA. In the same slice paired pulse facilitation (PPF) was evoked by a 50ms inter stimulus interval (ISI). Frequency facilitation (ff) of mossy fibers was measured by switching stimulation frequency from 0.1Hz to 1Hz. Only slices with robust ff were used for mf-long-term potentiation (LTP) recordings. LTP was induced by theta burst stimulation (TBS) at 30-40% of the maximum stimulus intensity. TBS consisted of a series of 10 bursts at 5Hz with 5 pulses per burst at 100Hz, delivered four times with 5s intervals. At the end of each recording 5μM DCGIV (Tocris Biosciences) was applied for at least 5min, if the fEPSP slope was not reduced for at least 50% slices were excluded from mf analysis.

Statistics: Statistical comparison of means in I/O, ff and LTP recordings between Tau-transgenic and control slices were accomplished by repeated measure ANOVA. In LTP measurements the last 10min of recording time were compared. PPR and the last 10min of LTP recording of pro-aggregant ON and anti-aggregant ON mice were compared by Student ´s t-test.

For further details see supplemental online information.

Results

Quantification of Tau expression by bioluminescence imaging

Pro- and anti-aggregant hTau40 variants (Fig. 1) are expressed simultaneously with a luciferase reporter gene under control of the bidirectional transactivator (tTA)-responsive promoter (P_{tet}bi-1). Therefore luciferase expression serves as a direct measure for Tau levels. Crossbreeding of pro- and anti-aggregant hTau40 strains with the CaMKIIα-tTA strain [45]

results in bigenic offspring with inducible expression (Tet-OFF system; [23]) of hTau40 and luciferase restricted to the forebrain as initially described in [19].

Previously, we had observed that expression levels of human Tau in pro- and anti-aggregant mice can vary between individuals and thus affect the extent of Tau pathology. To assure comparable expression levels of hTau40, we quantified the transgene expression strength of each individual prior to experiments by *in vivo* bioluminescence imaging (BLI), a non-invasive technique to visualize biomolecular processes in living organisms (for review; [13]). We detected a robust BLI signal emitted from the forebrain of pro- and anti-aggregant hTau40 mice, when gene expression was switched-ON (Fig. 2a1, a5, b). By contrast BLI signal intensities strongly decreased within 1-4 days when transgene expression was subsequently switched-OFF by doxycycline (Fig. 2a2-a4, a6-a8, b). A comparison of BLI signals and Tau protein levels revealed that BLI signal intensities > $1x10^7$ p/s corresponded to a ~2-fold overexpression of hTau40 over mouse Tau (mTau) in both pro- and anti-aggregant hTau40 mice at 16 months of gene expression (pro-ON, anti-ON, Fig. 2c, d). Consequently, individuals with BLI signal intensities > $1x10^7$p/s were selected for further experiments. Due to a shorter half-life time of luciferase (~3h, [29,75]) in comparison to Tau (~12-14h, [15]; ~60h, [57]), luciferase signals detected by BLI decreased within 1-4 days after switch-OFF (Fig. 2b), while human Tau was still present in brain homogenates for 2-4 weeks (Fig. 3b). However, 4 months after addition of doxycycline (pro-ON/OFF, anti-ON/OFF) total pro- and anti-aggregant hTau40 was depleted from homogenates of cortex tissue as demonstrated by immunoblotting using the human Tau specific antibody TauY9 (Fig. 2c).

Moreover TauY9 stainings revealed a mosaic-like expression pattern of hTau40 on pro-ON mice. At 16 months ON, hTau40 was located in cell bodies and apical dendrites of hippocampal and cortical neurons (Fig. 2e2, e7; arrows and arrowheads), clearly indicating missorting of Tau. Interestingly, cell somata of CA3 neurons and fibers located in the *stratum lucidum* showed the strongest staining intensities (Fig. 2e2; arrows and star). In *stratum lucidum,* apical dendrites of CA3 neurons are connected to mossy fibers of granule cells located in the dentate gyrus. In contrast, a more diffuse distribution of anti-aggregant hTau40 with less pronounced mislocalization of Tau was observed (Fig. 2e4, e9). Switching-OFF gene expression for 4 months resulted in a strong reduction of human Tau immunoreactivity in cortical and hippocampal neurons of pro-ON/OFF mice (Fig. 2e3, e8). However, some pro-aggregant hTau40 immunoreactivity was still detectable in *stratum lucidum* (Fig. 2e3; star). By contrast, a complete clearance of anti-aggregant hTau40 mice was observed in anti-ON/OFF mice (Fig. 2e5, e10).

Pathological changes related to the expression of pro-aggregant hTau40

As described earlier, pro-ON but not anti-ON mice develop an AD-like pathology, which is exacerbated with increasing age and can be partly reversed after switch-OFF [19]. At 16 months of hTau40 expression a separation of hTau40 and mTau by electrophoresis and subsequent immunoblotting demonstrated phosphorylation of exogenous hTau40 but also of endogenous mTau, predominantly in hippocampus homogenates of pro-ON mice (Fig. 3a). Interestingly, phosphorylation of hTau40 at sites located inside or in close vicinity to the four repeat domain (12E8, PHF-1, AT180) was particularly strong in comparison to the AT8

epitope, located in the projecting domain of Tau (Fig. 3a). The changes in antibody reactions between the different Tau forms and mouse lines were not uniform, possibly because of conformational changes of Tau and differential kinase activities. Immunohistochemical stainings manifested the presence of conformationally changed (MC1 epitope) and phosphorylated Tau (epitopes 12E8, PHF-1, AT180) in hippocampal and cortical neurons of pro-ON mice. Staining patterns once more pointed towards a massive missorting of Tau to cell bodies and apical dendrites (supplemental Fig. S1, S2). Again, Tau immunoreactivity was most pronounced in the hippocampal CA3 region and in *stratum lucidum* (supplemental Fig. S1, S2). In contrast to the western blot data, no AT8 positive neurons were detected (data not shown). After 4 months OFF, the pathological conformation as well as phosphorylation of hTau40 was mostly reversed in pro-ON/OFF mice as demonstrated by immunoblotting and histology. Only a weak Tau labeling outside neuronal cell bodies was still visible (supplemental Fig. S1, S2), reflecting the amount of phosphorylated mouse Tau, which was obviously leftover (Fig. 3a).

In addition, expression of pro-aggregant hTau40 led to co-aggregation of hTau40 and mTau, which was clearly detectable in the sarcosyl-insoluble fraction (Fig. 3c and supplemental Fig. S3b). However, only one mouse out of the experimental pro-ON group (16 months ON) displayed rare Gallyas-silver-positive hippocampal neurons, predominantly detected in the CA3 region of the hippocampus (data not shown).

To determine the clearance timeframe of soluble and insoluble Tau species from brains of pro-aggregant mice, we performed sarcosyl-extraction at 0.5, 1, 2 and 4 months after suppression of gene expression. Despite the fact that gene expression was inhibited within a few days, as demonstrated by BLI measurements (Fig. 2a, b), soluble hTau40 persisted for ~2-4 weeks but was clearly diminished 1 month after switch-OFF. As expected, switching-OFF hTau40 did not influence the soluble mouse Tau levels (Fig. 3b). Similarly, sarcosyl-insoluble co-aggregates consisting of pro-aggregant hTau40 and mTau were detected only 0.5 and 1 month after switch-OFF. Thereafter, hTau40 disappeared from the insoluble fraction, whereas the insoluble mTau persisted over several months but tended to decrease gradually (Fig. 3c).

Neuronal loss was not apparent inside the hippocampal formation in any of the analyzed mice at 16 months ON, although minor changes in the neuronal integrity cannot be excluded without quantification (Fig. 4). Nevertheless, a consistent reduction of pre- and postsynaptic proteins (synaptophysin, PSD95 and GluR1) by ~40% relative to controls (100%) was detected in hippocampus homogenates of pro-ON mice at 12 months of hTau40 expression (Fig. 5a, b). Moreover the regional distribution of synaptophysin was significantly reduced in the CA1 and CA3 area and in the dentate gyrus (DG) of pro-ON mice in comparison to age-matched controls (Fig. 5c, d), indicating a loss of synapses. Synaptic decay upon expression of pro-aggregant hTau40 was demonstrated previously by electron microscopy [19] and was now confirmed and extended by Golgi-staining of neurons with subsequent quantification of dendritic spines before and after switch-OFF (Fig. 6). It turned out that spine densities in pro-ON mice were significantly reduced on apical dendrites of CA1 pyramidal neurons relative to controls (Fig. 6b). Importantly, switching OFF pro-aggregant hTau40 for 4 months completely rescued synaptic protein levels (Fig. 5a, b) and resulted in a

Europe PMC Funders Author Manuscripts

partial recovery of spine numbers (Fig. 6a, b), indicating the reconstitution of functional synapses.

By contrast, most pathological changes are absent in mice expressing anti-aggregant hTau40 for 16 months. Anti-ON mice neither showed a pathological Tau conformation nor sarcosyl-insoluble Tau (supplemental Fig. S1, S3b). However, moderate phosphorylation of anti-aggregant hTau40 and mTau was observed in hippocampal homogenates, especially at the 12E8 epitope (Fig. 3a). In addition a few cell bodies inside the pyramidal layer of the hippocampus and in the somatosensory cortex (SSCx) were 12E8 and AT180 positive (supplemental Fig. S1, S2) indicating the presence of missorted, phosphorylated Tau species in anti-ON mice. Anti-ON mice did not display a reduction of postsynaptic proteins PSD95 and GluR1 in comparison to controls (Fig. 5a, b). However, a decrease of ~23% was observed for the presynaptic marker synaptophysin (Fig. 5b). Immunofluorescent labeling confirmed a decrease of synaptophysin in CA3, CA1 and DG (Fig. 5d). In contrast no alterations in apical spine densities of CA1 pyramidal neurons were observed (Fig. 6a, b). Switching-OFF anti-aggregant hTau40 expression for 4 months reversed all minor pathological changes. As expected, non-transgenic age-matched littermates displayed no signs of Tau pathology. Only minor amounts of phosphorylated mTau (12E8 and PHF-1) were present in hippocampus homogenates at the age of 16 months (Fig. 3a).

Cognitive impairment induced by pro-aggregant hTau40

No neuromotor changes in transgenic mice—It is of particular interest to test for neuromotor deficiencies because these problems have been reported for earlier generations of Tau-transgenic mice, to the extent that it made cognitive testing impossible [66]. Therefore pro- and anti-aggregant hTau40 mice were tested on grip strength as well as rotarod and activity. These measures did not differ between genotypes ($P > 0.05$ for all comparisons; Table 1).

Learning and memory deficits in pro-aggregant hTau40 mice are reversible—Pro-ON mice with 16 months of gene expression exhibited severe cognitive deficits in the Morris water maze (MWM) and in a passive avoidance learning paradigm (PA). Importantly, these deficits were completely reversible after switching human Tau OFF for 4 months (Fig. 7a, b). Regarding escape latency and path length in the MWM, pro-ON mice were considerably slower to reach the hidden platform in comparison to pro-ON/OFF (12 months ON + 4 months OFF), anti-ON (16 months ON), anti-ON/OFF (12 months ON + 4 months OFF) or age-matched control groups (Fig. 7a). Furthermore, pro-ON mice performed worse in MWM escape latency and path length from day 2 onwards (pairwise comparisons between pro-ON and the other 5 groups at four time points, $p < 0.001$). Swimming velocity did not differ between groups ($p > 0.05$ for all comparisons), thus it can be excluded that differences in the learning rate were due to a difference in neuromotor disability. Two days after the acquisition phase, a probe trial revealed no memory-related differences between the groups that finished acquisition training ($p > 0.05$ for all comparisons, data not shown).

PA was tested in the two-compartment step-through box. The test measures the ability of an animal to remember a mild foot-shock when entering a dark compartment. In comparison to

controls, pro-ON mice re-entered the dark compartment much faster, presumably because of impaired memory (Fig. 7b). More interestingly, pro-ON/OFF mice now shied away from the dark compartment, indicating that avoidance learning recovered after switching-OFF hTau40 expression. By contrast, the expression of anti-aggregant hTau40 had no impact on contextual learning and memory performance in PA (Fig. 7b).

Expression of pro-aggregant hTau40 causes synaptic dysfunction in the hippocampus

Impairments of CA1 Schaffer collateral plasticity—To determine physiological conditions underlying impairments in memory acquisition, we examined basal synaptic transmission, short term plasticity and long term plasticity (LTP) in area CA1 of acute hippocampal slices. Pro-ON mice (16 months ON) were compared to pro-ON/OFF (12 months ON + 4 months OFF) and age-matched controls. Anti-ON (16 months ON) animals were compared to anti-ON/OFF (12 months ON + 4 months OFF) and controls (Tab. 2).

No significant differences in basal synaptic transmission by stimulation of the Schaffer collateral-CA1 pathway were detected comparing all four transgenic groups to controls (Fig. 8a, b). We used paired-pulse ratio (PPR) analysis to determine presynaptic changes and did not find any differences between transgenic mice and controls (supplemental Fig. S4). Finally we induced CA1 LTP by theta burst stimulation (TBS) lasting up to 4 hours. Post tetanic potentiation (PTP), a measure of presynaptic calcium dynamics, was analyzed by comparing the first minute after TBS. It turned out that pro-ON mice displayed a reduced PTP compared to controls, which was not rescued by switching-OFF transgene expression for 4 months (Fig. 8c). To our surprise expression of anti-aggregant hTau40 led to an enhanced PTP, which was also not reversed after switch-OFF (Fig. 8d).

Looking at the last minutes of 4 hours of LTP recording, the Schaffer collateral-CA1 synapse was not potentiated in pro-ON mice in comparison to baseline values. At the end of LTP recordings the mean field excitatory postsynaptic potential (fEPSP) of pro-ON mice was significantly reduced relative to controls (Fig. 8c). Remarkably, LTP induction was completely restored in pro-ON/OFF mice (Fig. 8c). In contrast LTP in anti-ON mice was significantly enhanced compared to controls, whereas this enhancing tendency was reversed in anti-ON/OFF mice (Fig. 8d).

Functional constraints in the CA3 mossy fiber synapse—As described, the expression of pro-aggregant hTau40 results in a profound Tau pathology predominantly in CA3 neurons and in *stratum lucidum*. Therefore electrophysiological properties of the CA3 area were of particular interest (Tab. 3). This region mainly contains mossy fibers (mf), projecting from dentate gyrus granule cells to CA3 pyramidal neurons.

Stimulation of the mf-pathway in the hilus region by application of 10-100μA revealed a mean fEPSP slope of 252.2 ± 9.4 mV/s (n = 10) in 12 months old control mice. By contrast the mean fEPSP slope was strongly reduced to 128.2 ± 7.3 mV/s in pro-ON mice (12 months ON, n = 10; Fig. 9a1). Remarkably, we found a significant reduction of the fEPSP slope over the whole stimulation range in pro-ON mice, whereas pro-ON/OFF mice (8 months ON + 4 months OFF) were comparable to age-matched controls (Fig. 9a2). No

differences in input/output (I/O) curves were detected between anti-ON (12 months ON) and anti-ON/OFF animals (8 months ON + 4 months OFF) and controls (Fig. 9a3).

We used an inter stimulus interval (ISI) of 50ms to monitor changes in PPR. Of note, pro-ON mice demonstrated significantly decreased paired pulse facilitation (PPF) relative to controls and to pro-ON/OFF mice. Anti-ON and anti-ON/OFF mice displayed no change in PPR compared to controls (Fig. 9b). Among the most prominent features of mf-plasticity is frequency facilitation (ff), which occurs when the stimulus frequency is switched from 0.1Hz to 1Hz [53]. Frequency facilitation was significantly attenuated in pro-ON as well as in anti-ON mice compared to controls. At the same time pro-ON/OFF and anti-ON/OFF mice were comparable to controls (Fig. 9c1, c2), illustrating that these Tau-induced functional changes were fully reversible.

Finally, we used a TBS protocol to induce LTP of the mf-pathway. The specificity for mf-plasticity recording was ascertained by applying the mGluR group II blocker DCG IV at the end of each recording session (supplemental Fig. S5). Similar to LTP measurements in the CA1 region, the strongest effect on mf-LTP was observed in pro-ON mice. In these animals, mf-LTP was no longer inducible (Fig. 10a1). Surprisingly, mf-LTP of anti-ON mice was also significantly attenuated in comparison to the control group (Fig. 10a2). However, a direct comparison of pro-ON and anti-ON mf-fEPSP slopes revealed a significantly stronger mf-LTP reduction in pro-ON mice (Fig. 10b). Again, switching-OFF gene expression for 4 months resulted in a complete recovery of mf-LTP to control levels in pro-ON/OFF mice as well as in anti-ON/OFF mice (Fig. 10a1, a2, b).

Discussion

Reversibility of Tau-induced pathological changes

In the present study, we aimed to characterize effects of inducible pro- and anti-aggregant hTau40 on cognition and synaptic plasticity and their reversibility after switch-OFF. To avoid variations in exogenous Tau expression levels, which might impact on the severity of Tau-induced pathological changes, we used *in vivo* bioluminescence imaging (BLI) to select cohorts of mice with a consistent ~2-fold overexpression of exogenous hTau40 over endogenous mTau (Fig. 2). In spite of this low level of overexpression, pro-aggregant hTau40 exhibited pronounced consequences for Tau-induced pathological changes and more importantly for behavior and synaptic plasticity. Remarkably, most changes were completely reversible after switching-OFF the toxic mutant for 4 months. By contrast, no AD-like pathology was observed in mice expressing anti-aggregant hTau40, suggesting that pathological changes are not due to overexpression of exogenous Tau species.

Expression of pro-aggregant hTau40 caused a conformational change, missorting and phosphorylation of Tau and induced the formation of sarcosyl-insoluble co-aggregates composed of exogenous hTau40 and endogenous mTau (Fig. 3). As demonstrated earlier, the fraction of insoluble Tau increases with age [19] in parallel to synaptic damage and cognitive impairment. However Gallyas-silver or thioflavin-S positive cells occurred only sporadically in old individuals with high pro-aggregant hTau40 expression. No neurofibrillary tangles (NFTs) were detectable by means of electron microscopy in the

hippocampus of these mice (unpublished data). This is in clear contrast to our pro-aggregant Tau_{RD} model, with massive accumulation of Gallyas-positive neurons (already at 3 months of age) and presence of Tau filaments detected by negative stain electron microscopy [47,68]. Therefore we argue that sarcosyl-insoluble material composed of exogenous hTau40 and endogenous mTau may be considered as early pretangles (Tau oligomers or loosely packed aggregates that stain with diagnostic Tau antibodies but not with Gallyas silver), whereas true filaments or “full-blown” tangles are mostly absent in the hippocampus of pro-aggregant hTau40 mice.

Nevertheless, mechanisms of Tau aggregation are comparable in both models. As soon as pro-aggregant human Tau was switched-OFF, it slowly disappeared from the insoluble fraction, as old aggregates were in a constant turnover and pro-aggregant Tau was not replenished. In contrast, insoluble mTau persisted until the end of experiments (Fig. 3), presumably because it was still capable to incorporate into existing nuclei and thus creating new aggregates. Whether the aggregation of endogenous mouse Tau can be completely abolished remains to be investigated in future experiments with switch-OFF periods > 4 months. The results argue that Tau aggregates are not a rigid accumulation of amyloidogenic proteins but highly dynamic structures, which can change their composition because they are in a constant turnover with their subunits [16,68].

The less severe tau histopathology in pro-aggregant hTau40 mice in comparison to Tau_{RD} may be explained by its lower β-propensity and better binding to microtubules (MTs). The critical sequences determining Tau´s propensity for β-structure are two hexapeptide motifs inside the repeat domain [77]. Mutations such as P301L or ΔK280 accelerate Tau aggregation (pro-aggregant), whereas additional insertion of two prolines (I277P and I308P) abrogates the formation of β-structures (anti-aggregant) [34,77]. Tau_{RD} represents the “naked” four repeat domain of Tau lacking the adjacent flanking domains, which promote MT-binding [51]. Consequently, Tau_{RD} does not bind to MTs [27] and the exposed β-structures can efficiently trigger the aggregation process in the neuronal cytosol. By contrast the “β-structure burden” in mice expressing pro-aggregant hTau40 is lower, because hTau40 still binds to MTs.

Spatial and contextual memory defects recover after switch-OFF of human Tau

Tau-related pathological changes predominantly affect the hippocampal formation in pro-aggregant hTau40 mice, especially the CA3 region. The hippocampus plays an important role in spatial and contextual learning processes and memory consolidation after initial acquisition [18]. To examine hippocampus dependent learning and memory, we used the Morris water maze test and a passive avoidance paradigm [52,67]. Pro-ON mice exhibited longer path lengths to reach the hidden platform (Fig. 7), which serves as a measure of cognitive performance [25]. Since pro-ON mice did not show any impairment in neuromotor performance, the acquisition deficits cannot be ascribed to an undetected motor phenotype, which developed frequently in mutant mice expressing Tau in the spinal cord [1,30,31,42,66,81].

Pro-ON mice also failed to remember the electric shock, which was applied in the dark compartment of the passive avoidance box the day before (Fig. 7), indicating impaired

associative memory of these mice. Comparable effects of Tau-pathology on spatial and contextual learning impairments are observed for mice expressing the pro-aggregant Tau repeat domain Tau_{RD} [69] and other AD mouse models [2,6,17,58,72]. All cognitive defects completely recovered after switching-OFF the toxic mutant for 4 months. By contrast, no cognitive deficits were observed in mice expressing anti-aggregant hTau40, suggesting that memory impairments are specifically related to pro-aggregant hTau40 species.

Pro-aggregant human Tau causes synaptic decay

Expression of pro-aggregant hTau40 caused a profound synaptic decay (Fig. 5) and loss of CA1 dendritic spines (Fig. 6) even though no neuronal death was detected (Fig. 4). Dendritic spines provide the structural prerequisites for excitatory synapse formation and hence modulation of synaptic plasticity [54]. Synapse loss has been identified as an important correlate of cognitive impairment in AD patients [12,73] and several AD mouse models present with early synaptic failure [6,55,70] and reduction or regression of dendritic spines [37,39,48,59].

The prominent reduction of synaptophysin levels in area CA3 of pro-ON and anti-ON mice (Fig. 5) correlated functionally with a reduction in paired pulse facilitation (PPF) and frequency facilitation (ff) in the mossy fiber (mf) tract (Fig. 9). All of these plasticity phenomena depend on presynaptic calcium dynamics and transmitter release [82] and were partly recovered after switch-OFF.

Basal synaptic transmission in Schaffer collateral CA1 was not affected in pro- and anti-aggregant hTau40 transgenic mice (Fig. 8). However basal synaptic transmission in mf of pro-ON mice was strongly impaired (Fig. 9), which is in contrast to our previous study with mice expressing pro-aggregant Tau_{RD} [69]. The difference of mf-excitability in both mouse-models of tauopathy may be explained by the disability of Tau_{RD} to bind to MTs [27]. We conclude that the observed mf-excitability impairment somehow involves the flanking regions or other domains of the Tau outside the repeats.

Short-term plasticity in CA1 of pro-ON mice was strongly attenuated, as demonstrated by reduced post tetanic potentiation (PTP), whereas in anti-ON mice PTP in CA1 was clearly enhanced (Tab. 2). Both, reduction and enhancement of CA1 short-term plasticity were not rescued after switch-OFF, demonstrating an irreversible, presynaptic effect of hTau40 in CA1. By contrast, the short-term plasticity in CA3 of pro-ON and anti-ON was significantly impaired as demonstrated by reduced frequency facilitation (ff, Fig. 9). Of note, a full recovery of ff was observed in CA3 after 4 months OFF (Fig. 9). Differences in short-term plasticity between CA1 and CA3 in hTau40 expressing mice may stem from different presynaptic mechanisms. One underlying presynaptic mechanism of PTP is the rising Ca^{2+} concentration in terminal boutons [71,78], which may disturb presynaptic Ca^{2+} dynamics in pro-ON and anti-ON mice. By contrast, mf short-term plasticity is specifically sensitive to adenosine [35].

Furthermore, LTP was strongly impaired in pro-ON mice in CA1 (Fig. 8) as well as in CA3 (Fig. 10), which is in agreement with spatial cognitive defects and reduced spine densities in these animals. Similar to memory and spines, LTP recovered after switch-OFF of pro-

aggregant hTau40. CA3-LTP in anti-ON mice was slightly reduced relative to controls (Fig. 10), reflecting a mild impairing synaptic effect of anti-aggregant hTau40. In contrast, LTP in CA1 of anti-ON mice was enhanced compared to controls (Fig. 9). These opposing effects of anti-aggregant hTau40 in CA1 and CA3 may be explained by regional differences of Schaffer collateral-CA1 and mf-CA3 plasticity mechanisms. While CA1-Schaffer collateral LTP mainly depends on postsynaptic mechanisms, CA3-mossy fiber LTP is predominantly influenced by presynaptic mechanisms [53]. However, the enhancing effect of anti-aggregant Tau in CA1-LTP needs further investigation in future studies.

Synaptotoxicity correlates to β-structures, not to NFTs

Despite a less pronounced Tau pathology without neuronal loss and NFTs in the hippocampus, pro-aggregant hTau40 mice develop severe defects in synaptic plasticity and cognition similar to other mouse models with massive NFTs formation and neuronal loss. Suppression of exogenous Tau expression in these models improves cognition, while NFT pathology continues [58,62,69]. We conclude that not Tau tangles but smaller entities such as soluble oligomers disrupt cognition and synaptic transmission. This hypothesis has been supported by other studies. No functional or structural differences were detected between NFT-positive and NFT-negative neurons [60] and Tau oligomers occur in AD brains and correlate with Tau-induced changes [11,61]. Memory loss in rTg4510 mice correlates to the level of soluble Tau oligomers [5] and neurons can tolerate NFTs over long periods [16] and appear functionally active [20]. Although a considerably higher phosphorylation of pro-aggregant hTau40 than in anti-aggregant hTau40 mice was observed, we argue against hyperphosphorylation as main cause of cognitive and synaptic dysfunction. This view is based on our previous observations with mice expressing Tau_{RD}, which lacks most of the pathological phosphorylation sites yet shows pronounced aggregation and synaptic damage [69].

How could toxic soluble Tau species impact on cognition and synaptic transmission? Normally Tau is localized mainly in axons [7–9,36], stabilizing MTs and regulating axonal transport processes. Detachment of Tau from MTs as a consequence of phosphorylation, results in transport alterations and missorting of Tau [24,74], which may affect pre- and postsynaptic sites. Injection of human Tau into presynaptic terminals of the squid giant synapse led to a rapid synaptic transmission block and induced clustering of synaptic vesicles and hence disturbances of presynaptic transmitter release dynamics [49]. Missorting of Tau into dendrites and spines compromised transport of mitochondria, leading to the breakdown of MTs and the decay of spines [80]. Phosphorylated Tau within dendritic spines might impair synaptic transmission by decreasing AMPA and NMDA receptor densities [28]. Recently, a scaffolding function of Tau in the postsynapse was proposed, whereby Tau interacts with the tyrosine kinase fyn via the projection domain and recruits fyn to postsynaptic sites [32,40].

Our data highlight that toxicity – especially “synaptotoxicity” - is related to the aggregation process and to β-structures but not necessarily to the presence of neurofibrillary tangles (NFTs). Importantly, functional deficits can be reversed by reducing aggregation-prone Tau species. Our mouse model mimics an early stage of AD and offers potential to evaluate new

therapeutic strategies and drug candidates according to their benefit on cognitive functions. In this context strategies reducing soluble Tau species by enforcing protein degradation systems (e.g. autophagy, [38]) or substances which counteract the aggregation process [10,56] seem to be promising.

Supplementary Material

Refer to Web version on PubMed Central for supplementary material.

Acknowledgements

We thank Dr. A. Haemisch and his team at the animal facility at the University of Hamburg Medical School for their continuous help in mouse breeding, O. Petrova and S. Hahn for their excellent technical assistance, Dr. A. Marx (Max-Planck Unit for Structural Molecular Biology, Hamburg, Germany) for advice on statistics and Dr. G. Glassmeier (University of Hamburg Medical School) for technical advice on electrophysiology. We gratefully acknowledge reagents from Prof. Dr. E. Kandel (Columbia University, New York, NY; CaMKIIα-tTA transgenic mice), Dr. P. Seubert (Elan Pharma, South San Francisco, CA; 12E8 antibody) and Dr. P. Davies (Albert Einstein College, Bronx, NY; MC-1 and PHF-1 antibodies). This research was supported by MPG, DZNE, BMBF/KNDD, Wellcome Trust/MRC, Metlife Foundation (to E.M.M.), EU-FP7/Memosad (Grant No. 2006121 to E.M.M. and R. D'H), FWO-Vlaanderen (grant G.0327.08 to D.B. and R. D'H; and an FWO junior scholarship to A.VdJ).

Abbreviations

hTau40	human full-length Tau
CaMKIIα	calcium/calmodulin-dependent protein kinase IIα
BLI	bioluminescence imaging
LTP	long-term potentiation
AD	Alzheimer´s disease
NFT	neurofibrillary tangle
MT	microtubule
PHF	paired helical filament
FTD	frontotemporal dementia
FTDP-17	frontotemporal dementia with parkinsonism linked to chromosome 17
CNS	central nervous system
tTA	tetracycline transactivator
pro-ON	transgenic mice expressing pro-aggregant full-length hTau40 (12-16 months ON)
pro-ON/OFF	transgenic mice expressing pro-aggregant hTau40, then switched-OFF (8-12 ON + 4 months OFF)
ATP	adenosine triphosphate

Europe PMC Funders Author Manuscripts

Europe PMC Funders Author Manuscripts

ROI	region of interest
mf	mossy fiber
NeuN	neuronal nuclei
PSD95	postsynaptic density 95
GluR1	glutamate receptor 1
SSCx	somatosensory cortex
MWM	Morris water maze
PA	passive avoidance
PPF	paired-pulse facilitation
PPR	paired-pulse ratio
ISI	inter stimulus interval
TBS	theta burst stimulation
PTP	post tetanic potentiation
fEPSP	field excitatory postsynaptic potential
I/O	input/output
ff	frequency facilitation
AMPA	α-amino-3-hydroxy-5-methyl-4-isoxazolepropionic acid
NMDA	N-methyl D-aspartate

References

1. Allen B, Ingram E, Takao M, Smith MJ, Jakes R, Virdee K, Yoshida H, Holzer M, Craxton M, Emson PC, Atzori C, et al. Abundant tau filaments and nonapoptotic neurodegeneration in transgenic mice expressing human P301S tau protein. J Neurosci. 2002; 22(21):9340–9351. [PubMed: 12417659]
2. Arendash GW, Lewis J, Leighty RE, McGowan E, Cracchiolo JR, Hutton M, Garcia MF. Multi-metric behavioral comparison of APPsw and P301L models for Alzheimer's disease: linkage of poorer cognitive performance to tau pathology in forebrain. Brain Res. 2004; 1012(1-2):29–41. [PubMed: 15158158]
3. Ballatore C, Lee VM, Trojanowski JQ. Tau-mediated neurodegeneration in Alzheimer's disease and related disorders. Nat Rev Neurosci. 2007; 8(9):663–672. [PubMed: 17684513]
4. Behrens CJ, van den Boom LP, de Hoz L, Friedman A, Heinemann U. Induction of sharp wave-ripple complexes in vitro and reorganization of hippocampal networks. Nat Neurosci. 2005; 8(11): 1560–1567. [PubMed: 16222227]
5. Berger Z, Roder H, Hanna A, Carlson A, Rangachari V, Yue M, Wszolek Z, Ashe K, Knight J, Dickson D, Andorfer C, et al. Accumulation of pathological tau species and memory loss in a conditional model of tauopathy. J Neurosci. 2007; 27(14):3650–3662. [PubMed: 17409229]

Europe PMC Funders Author Manuscripts

6. Billings LM, Oddo S, Green KN, McGaugh JL, LaFerla FM. Intraneuronal Abeta causes the onset of early Alzheimer's disease-related cognitive deficits in transgenic mice. Neuron. 2005; 45(5):675–688. [PubMed: 15748844]
7. Binder LI, Frankfurter A, Rebhun LI. The distribution of tau in the mammalian central nervous system. J Cell Biol. 1985; 101(4):1371–1378. [PubMed: 3930508]
8. Brion JP, Guilleminot J, Couchie D, Flament-Durand J, Nunez J. Both adult and juvenile tau microtubule-associated proteins are axon specific in the developing and adult rat cerebellum. Neuroscience. 1988; 25(1):139–146. [PubMed: 3134623]
9. Brion JP, Guilleminot J, Nunez J. Dendritic and axonal distribution of the microtubule-associated proteins MAP2 and tau in the cerebellum of the nervous mutant mouse. Brain Res Dev Brain Res. 1988; 44(2):221–232. [PubMed: 3147150]
10. Bulic B, Pickhardt M, Mandelkow EM, Mandelkow E. Tau protein and tau aggregation inhibitors. Neuropharmacology. 2010; 59(4-5):276–289. [PubMed: 20149808]
11. Clavaguera F, Bolmont T, Crowther RA, Abramowski D, Frank S, Probst A, Fraser G, Stalder AK, Beibel M, Staufenbiel M, Jucker M, et al. Transmission and spreading of tauopathy in transgenic mouse brain. Nat Cell Biol. 2009; 11(7):909–913. [PubMed: 19503072]
12. Coleman PD, Yao PJ. Synaptic slaughter in Alzheimer's disease. Neurobiology of aging. 2003; 24(8):1023–1027. [PubMed: 14643374]
13. Contag CH. In vivo pathology: seeing with molecular specificity and cellular resolution in the living body. Annu Rev Pathol. 2007; 2:277–305. [PubMed: 18039101]
14. D'Hooge R, Lullmann-Rauch R, Beckers T, Balschun D, Schwake M, Reiss K, von Figura K, Saftig P. Neurocognitive and psychotiform behavioral alterations and enhanced hippocampal long-term potentiation in transgenic mice displaying neuropathological features of human alpha-mannosidosis. J Neurosci. 2005; 25(28):6539–6549. [PubMed: 16014715]
15. David DC, Layfield R, Serpell L, Narain Y, Goedert M, Spillantini MG. Proteasomal degradation of tau protein. J Neurochem. 2002; 83(1):176–185. [PubMed: 12358741]
16. de Calignon A, Fox LM, Pitstick R, Carlson GA, Bacskai BJ, Spires-Jones TL, Hyman BT. Caspase activation precedes and leads to tangles. Nature. 2010; 464(7292):1201–1204. [PubMed: 20357768]
17. Denk F, Wade-Martins R. Knock-out and transgenic mouse models of tauopathies. Neurobiol Aging. 2009; 30(1):1–13. [PubMed: 17590238]
18. Dudai Y. The neurobiology of consolidations, or, how stable is the engram? Annu Rev Psychol. 2004; 55:51–86. [PubMed: 14744210]
19. Eckermann K, Mocanu MM, Khlistunova I, Biernat J, Nissen A, Hofmann A, Schonig K, Bujard H, Haemisch A, Mandelkow E, Zhou L, et al. The beta-propensity of Tau determines aggregation and synaptic loss in inducible mouse models of tauopathy. J Biol Chem. 2007; 282(43):31755–31765. [PubMed: 17716969]
20. Fox LM, William CM, Adamowicz DH, Pitstick R, Carlson GA, Spires-Jones TL, Hyman BT. Soluble tau species, not neurofibrillary aggregates, disrupt neural system integration in a tau transgenic model. J Neuropathol Exp Neurol. 2011; 70(7):588–595. [PubMed: 21666499]
21. Glaser EM, Van der Loos H. Analysis of thick brain sections by obverse-reverse computer microscopy: application of a new, high clarity Golgi-Nissl stain. J Neurosci Methods. 1981; 4(2): 117–125. [PubMed: 6168870]
22. Goode BL, Feinstein SC. Identification of a novel microtubule binding and assembly domain in the developmentally regulated inter-repeat region of tau. J Cell Biol. 1994; 124(5):769–782. [PubMed: 8120098]
23. Gossen M, Bujard H. Studying gene function in eukaryotes by conditional gene inactivation. Annu Rev Genet. 2002; 36:153–173. [PubMed: 12429690]
24. Götz J, Ittner LM, Kins S. Do axonal defects in tau and amyloid precursor protein transgenic animals model axonopathy in Alzheimer's disease? J Neurochem. 2006; 98(4):993–1006. [PubMed: 16787410]
25. Graziano A, Petrosini L, Bartoletti A. Automatic recognition of explorative strategies in the Morris water maze. J Neurosci Methods. 2003; 130(1):33–44. [PubMed: 14583402]

26. Greenberg SG, Davies P. A preparation of Alzheimer paired helical filaments that displays distinct tau proteins by polyacrylamide gel electrophoresis. Proc Natl Acad Sci U S A. 1990; 87(15):5827–5831. [PubMed: 2116006]
27. Gustke N, Trinczek B, Biernat J, Mandelkow EM, Mandelkow E. Domains of tau protein and interactions with microtubules. Biochemistry. 1994; 33(32):9511–9522. [PubMed: 8068626]
28. Hoover BR, Reed MN, Su J, Penrod RD, Kotilinek LA, Grant MK, Pitstick R, Carlson GA, Lanier LM, Yuan LL, Ashe KH, et al. Tau mislocalization to dendritic spines mediates synaptic dysfunction independently of neurodegeneration. Neuron. 2010; 68(6):1067–1081. [PubMed: 21172610]
29. Ignowski JM, Schaffer DV. Kinetic analysis and modeling of firefly luciferase as a quantitative reporter gene in live mammalian cells. Biotechnol Bioeng. 2004; 86(7):827–834. [PubMed: 15162459]
30. Ikeda M, Shoji M, Kawarai T, Kawarabayashi T, Matsubara E, Murakami T, Sasaki A, Tomidokoro Y, Ikarashi Y, Kuribara H, Ishiguro K, et al. Accumulation of filamentous tau in the cerebral cortex of human tau R406W transgenic mice. Am J Pathol. 2005; 166(2):521–531. [PubMed: 15681835]
31. Ishihara T, Hong M, Zhang B, Nakagawa Y, Lee MK, Trojanowski JQ, Lee VM. Age-dependent emergence and progression of a tauopathy in transgenic mice overexpressing the shortest human tau isoform. Neuron. 1999; 24(3):751–762. [PubMed: 10595524]
32. Ittner LM, Ke YD, Delerue F, Bi M, Gladbach A, van Eersel J, Wolfing H, Chieng BC, Christie MJ, Napier IA, Eckert A, et al. Dendritic function of tau mediates amyloid-beta toxicity in Alzheimer's disease mouse models. Cell. 2010; 142(3):387–397. [PubMed: 20655099]
33. Jaworski T, Dewachter I, Seymour CM, Borghgraef P, Devijver H, Kugler S, Van Leuven F. Alzheimer's disease: old problem, new views from transgenic and viral models. Biochim Biophys Acta. 2010; 1802(10):808–818. [PubMed: 20332023]
34. Khlistunova I, Biernat J, Wang Y, Pickhardt M, von Bergen M, Gazova Z, Mandelkow E, Mandelkow EM. Inducible expression of Tau repeat domain in cell models of tauopathy: aggregation is toxic to cells but can be reversed by inhibitor drugs. J Biol Chem. 2006; 281(2): 1205–1214. [PubMed: 16246844]
35. Klausnitzer J, Manahan-Vaughan D. Frequency facilitation at mossy fiber-CA3 synapses of freely behaving rats is regulated by adenosine A1 receptors. J Neurosci. 2008; 28(18):4836–4840. [PubMed: 18448660]
36. Kowall NW, Kosik KS. Axonal disruption and aberrant localization of tau protein characterize the neuropil pathology of Alzheimer's disease. Ann Neurol. 1987; 22(5):639–643. [PubMed: 3122646]
37. Kremer A, Maurin H, Demedts D, Devijver H, Borghgraef P, Van Leuven F. Early Improved and Late Defective Cognition Is Reflected by Dendritic Spines in Tau.P301L Mice. The Journal of neuroscience : the official journal of the Society for Neuroscience. 2011; 31(49):18036–18047. [PubMed: 22159117]
38. Krüger U, Wang Y, Kumar S, Mandelkow EM. Autophagic degradation of tau in primary neurons and its enhancement by trehalose. Neurobiology of aging. 2011
39. Lanz TA, Carter DB, Merchant KM. Dendritic spine loss in the hippocampus of young PDAPP and Tg2576 mice and its prevention by the ApoE2 genotype. Neurobiol Dis. 2003; 13(3):246–253. [PubMed: 12901839]
40. Lee G, Newman ST, Gard DL, Band H, Panchamoorthy G. Tau interacts with src-family non-receptor tyrosine kinases. J Cell Sci. 1998; 111(Pt 21):3167–3177. [PubMed: 9763511]
41. Lee VM, Goedert M, Trojanowski JQ. Neurodegenerative tauopathies. Annu Rev Neurosci. 2001; 24:1121–1159. [PubMed: 11520930]
42. Lewis J, McGowan E, Rockwood J, Melrose H, Nacharaju P, Van Slegtenhorst M, Gwinn-Hardy K, Paul Murphy M, Baker M, Yu X, Duff K, et al. Neurofibrillary tangles, amyotrophy and progressive motor disturbance in mice expressing mutant (P301L) tau protein. Nat Genet. 2000; 25(4):402–405. [PubMed: 10932182]
43. Li X, Kumar Y, Zempel H, Mandelkow EM, Biernat J, Mandelkow E. Novel diffusion barrier for axonal retention of Tau in neurons and its failure in neurodegeneration. EMBO J. 2011

44. Mandelkow E, von Bergen M, Biernat J, Mandelkow EM. Structural principles of tau and the paired helical filaments of Alzheimer's disease. Brain Pathol. 2007; 17(1):83–90. [PubMed: 17493042]
45. Mayford M, Bach ME, Huang YY, Wang L, Hawkins RD, Kandel ER. Control of memory formation through regulated expression of a CaMKII transgene. Science. 1996; 274(5293):1678–1683. [PubMed: 8939850]
46. McGowan E, Eriksen J, Hutton M. A decade of modeling Alzheimer's disease in transgenic mice. Trends Genet. 2006; 22(5):281–289. [PubMed: 16567017]
47. Mocanu MM, Nissen A, Eckermann K, Khlistunova I, Biernat J, Drexler D, Petrova O, Schonig K, Bujard H, Mandelkow E, Zhou L, et al. The potential for beta-structure in the repeat domain of tau protein determines aggregation, synaptic decay, neuronal loss, and coassembly with endogenous Tau in inducible mouse models of tauopathy. J Neurosci. 2008; 28(3):737–748. [PubMed: 18199773]
48. Moolman DL, Vitolo OV, Vonsattel JP, Shelanski ML. Dendrite and dendritic spine alterations in Alzheimer models. J Neurocytol. 2004; 33(3):377–387. [PubMed: 15475691]
49. Moreno H, Choi S, Yu E, Brusco J, Avila J, Moreira JE, Sugimori M, Llinas RR. Blocking Effects of Human Tau on Squid Giant Synapse Transmission and Its Prevention by T-817 MA. Front Synaptic Neurosci. 2011; 3:3. [PubMed: 21629767]
50. Morris R. Developments of a water-maze procedure for studying spatial learning in the rat. J Neurosci Methods. 1984; 11(1):47–60. [PubMed: 6471907]
51. Mukrasch MD, Biernat J, von Bergen M, Griesinger C, Mandelkow E, Zweckstetter M. Sites of tau important for aggregation populate {beta}-structure and bind to microtubules and polyanions. The Journal of biological chemistry. 2005; 280(26):24978–24986. [PubMed: 15855160]
52. Nakazawa K, McHugh TJ, Wilson MA, Tonegawa S. NMDA receptors, place cells and hippocampal spatial memory. Nat Rev Neurosci. 2004; 5(5):361–372. [PubMed: 15100719]
53. Nicoll RA, Schmitz D. Synaptic plasticity at hippocampal mossy fibre synapses. Nat Rev Neurosci. 2005; 6(11):863–876. [PubMed: 16261180]
54. Nimchinsky EA, Sabatini BL, Svoboda K. Structure and function of dendritic spines. Annu Rev Physiol. 2002; 64:313–353. [PubMed: 11826272]
55. Oddo S, Caccamo A, Shepherd JD, Murphy MP, Golde TE, Kayed R, Metherate R, Mattson MP, Akbari Y, LaFerla FM. Triple-transgenic model of Alzheimer's disease with plaques and tangles: intracellular Abeta and synaptic dysfunction. Neuron. 2003; 39(3):409–421. [PubMed: 12895417]
56. Pickhardt M, Larbig G, Khlistunova I, Coksezen A, Meyer B, Mandelkow EM, Schmidt B, Mandelkow E. Phenylthiazolyl-hydrazide and its derivatives are potent inhibitors of tau aggregation and toxicity in vitro and in cells. Biochemistry. 2007; 46(35):10016–10023. [PubMed: 17685560]
57. Poppek D, Keck S, Ermak G, Jung T, Stolzing A, Ullrich O, Davies KJ, Grune T. Phosphorylation inhibits turnover of the tau protein by the proteasome: influence of RCAN1 and oxidative stress. Biochem J. 2006; 400(3):511–520. [PubMed: 16939415]
58. Ramsden M, Kotilinek L, Forster C, Paulson J, McGowan E, SantaCruz K, Guimaraes A, Yue M, Lewis J, Carlson G, Hutton M, et al. Age-dependent neurofibrillary tangle formation, neuron loss, and memory impairment in a mouse model of human tauopathy (P301L). J Neurosci. 2005; 25(46):10637–10647. [PubMed: 16291936]
59. Ricobaraza A, Cuadrado-Tejedor M, Marco S, Perez-Otano I, Garcia-Osta A. Phenylbutyrate rescues dendritic spine loss associated with memory deficits in a mouse model of Alzheimer disease. Hippocampus. 2010
60. Rocher AB, Crimins JL, Amatrudo JM, Kinson MS, Todd-Brown MA, Lewis J, Luebke JI. Structural and functional changes in tau mutant mice neurons are not linked to the presence of NFTs. Exp Neurol. 2010; 223(2):385–393. [PubMed: 19665462]
61. Sahara N, Maeda S, Takashima A. Tau oligomerization: a role for tau aggregation intermediates linked to neurodegeneration. Curr Alzheimer Res. 2008; 5(6):591–598. [PubMed: 19075586]
62. Santacruz K, Lewis J, Spires T, Paulson J, Kotilinek L, Ingelsson M, Guimaraes A, DeTure M, Ramsden M, McGowan E, Forster C, et al. Tau suppression in a neurodegenerative mouse model improves memory function. Science. 2005; 309(5733):476–481. [PubMed: 16020737]

63. Scattoni ML, Gasparini L, Alleva E, Goedert M, Calamandrei G, Spillantini MG. Early behavioural markers of disease in P301S tau transgenic mice. Behav Brain Res. 2010; 208(1):250–257. [PubMed: 20004218]
64. Schindowski K, Bretteville A, Leroy K, Begard S, Brion JP, Hamdane M, Buee L. Alzheimer's disease-like tau neuropathology leads to memory deficits and loss of functional synapses in a novel mutated tau transgenic mouse without any motor deficits. Am J Pathol. 2006; 169(2):599–616. [PubMed: 16877359]
65. Selkoe DJ. The molecular pathology of Alzheimer's disease. Neuron. 1991; 6(4):487–498. [PubMed: 1673054]
66. Spittaels K, Van den Haute C, Van Dorpe J, Bruynseels K, Vandezande K, Laenen I, Geerts H, Mercken M, Sciot R, Van Lommel A, Loos R, et al. Prominent axonopathy in the brain and spinal cord of transgenic mice overexpressing four-repeat human tau protein. Am J Pathol. 1999; 155(6): 2153–2165. [PubMed: 10595944]
67. Sutherland RJ, McDonald RJ. Hippocampus, amygdala, and memory deficits in rats. Behav Brain Res. 1990; 37(1):57–79. [PubMed: 2310495]
68. Sydow A, Mandelkow EM. 'Prion-like' propagation of mouse and human tau aggregates in an inducible mouse model of tauopathy. Neurodegener Dis. 2010; 7(1–3):28–31. [PubMed: 20160454]
69. Sydow A, Van der Jeugd A, Zheng F, Ahmed T, Balschun D, Petrova O, Drexler D, Zhou L, Rune G, Mandelkow E, D'Hooge R, et al. Tau-induced defects in synaptic plasticity, learning, and memory are reversible in transgenic mice after switching off the toxic Tau mutant. J Neurosci. 2011; 31(7):2511–2525. [PubMed: 21325519]
70. Tampellini D, Rahman N, Gallo EF, Huang Z, Dumont M, Capetillo-Zarate E, Ma T, Zheng R, Lu B, Nanus DM, Lin MT, et al. Synaptic activity reduces intraneuronal Abeta, promotes APP transport to synapses, and protects against Abeta-related synaptic alterations. J Neurosci. 2009; 29(31):9704–9713. [PubMed: 19657023]
71. Tang Y, Zucker RS. Mitochondrial involvement in post-tetanic potentiation of synaptic transmission. Neuron. 1997; 18(3):483–491. [PubMed: 9115741]
72. Tatebayashi Y, Miyasaka T, Chui DH, Akagi T, Mishima K, Iwasaki K, Fujiwara M, Tanemura K, Murayama M, Ishiguro K, Planel E, et al. Tau filament formation and associative memory deficit in aged mice expressing mutant (R406W) human tau. Proc Natl Acad Sci U S A. 2002; 99(21): 13896–13901. [PubMed: 12368474]
73. Terry RD, Masliah E, Salmon DP, Butters N, DeTeresa R, Hill R, Hansen LA, Katzman R. Physical basis of cognitive alterations in Alzheimer's disease: synapse loss is the major correlate of cognitive impairment. Ann Neurol. 1991; 30(4):572–580. [PubMed: 1789684]
74. Thies E, Mandelkow EM. Missorting of tau in neurons causes degeneration of synapses that can be rescued by the kinase MARK2/Par-1. The Journal of neuroscience : the official journal of the Society for Neuroscience. 2007; 27(11):2896–2907. [PubMed: 17360912]
75. Thompson JF, Hayes LS, Lloyd DB. Modulation of firefly luciferase stability and impact on studies of gene regulation. Gene. 1991; 103(2):171–177. [PubMed: 1889744]
76. van Swieten JC, Bronner IF, Azmani A, Severijnen LA, Kamphorst W, Ravid R, Rizzu P, Willemsen R, Heutink P. The DeltaK280 mutation in MAP tau favors exon 10 skipping in vivo. J Neuropathol Exp Neurol. 2007; 66(1):17–25. [PubMed: 17204933]
77. von Bergen M, Barghorn S, Li L, Marx A, Biernat J, Mandelkow EM, Mandelkow E. Mutations of tau protein in frontotemporal dementia promote aggregation of paired helical filaments by enhancing local beta-structure. J Biol Chem. 2001; 276(51):48165–48174. [PubMed: 11606569]
78. Wu LG, Saggau P. Presynaptic calcium is increased during normal synaptic transmission and paired-pulse facilitation, but not in long-term potentiation in area CA1 of hippocampus. J Neurosci. 1994; 14(2):645–654. [PubMed: 7905515]
79. Yoshiyama Y, Higuchi M, Zhang B, Huang SM, Iwata N, Saido TC, Maeda J, Suhara T, Trojanowski JQ, Lee VM. Synapse loss and microglial activation precede tangles in a P301S tauopathy mouse model. Neuron. 2007; 53(3):337–351. [PubMed: 17270732]

80. Zempel H, Thies E, Mandelkow E, Mandelkow EM. Abeta oligomers cause localized Ca(2+) elevation, missorting of endogenous Tau into dendrites, Tau phosphorylation, and destruction of microtubules and spines. J Neurosci. 2010; 30(36):11938–11950. [PubMed: 20826658]

81. Zhang B, Higuchi M, Yoshiyama Y, Ishihara T, Forman MS, Martinez D, Joyce S, Trojanowski JQ, Lee VM. Retarded axonal transport of R406W mutant tau in transgenic mice with a neurodegenerative tauopathy. J Neurosci. 2004; 24(19):4657–4667. [PubMed: 15140937]

82. Zucker RS, Regehr WG. Short-term synaptic plasticity. Annu Rev Physiol. 2002; 64:355–405. [PubMed: 11826273]

Europe PMC Funders Author Manuscripts

Europe PMC Funders Author Manuscripts

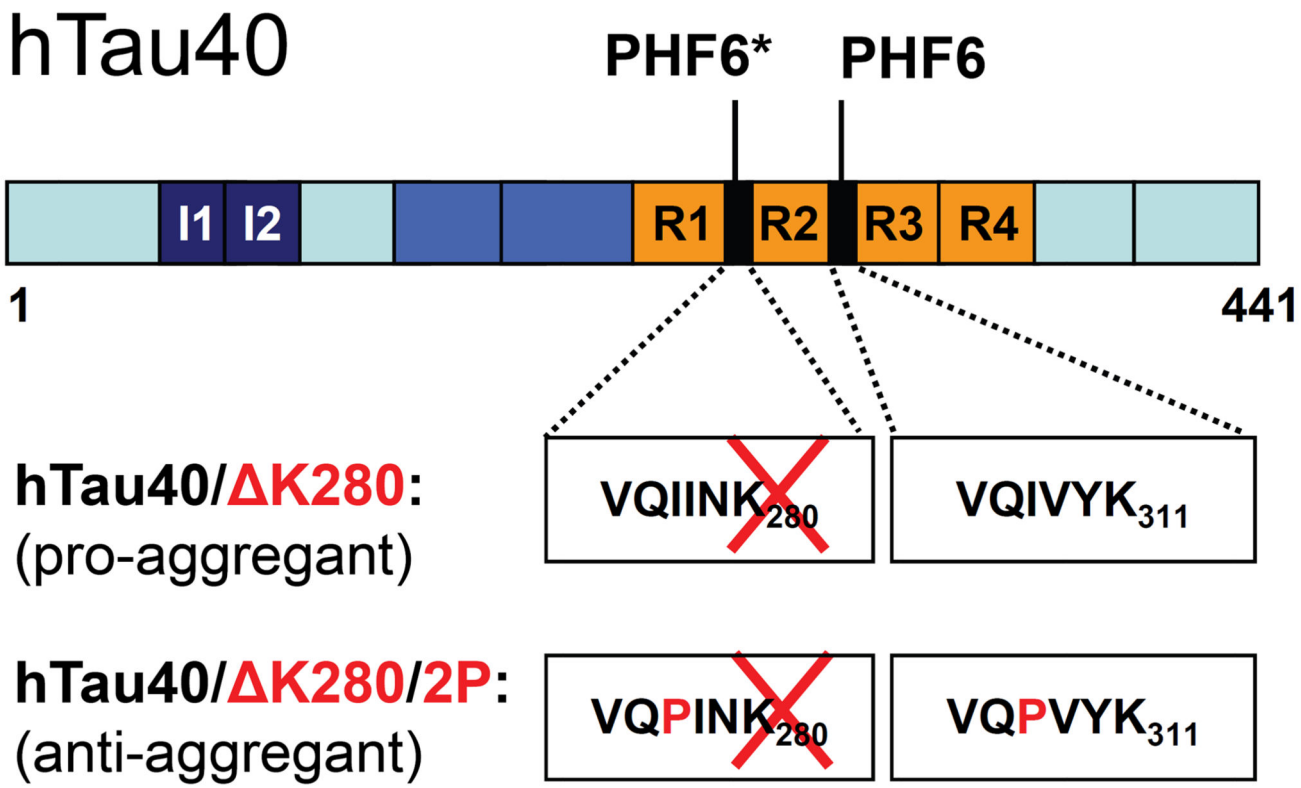

Fig. 1. Domains of human full-length Tau

Scheme representing the domains of human full-length Tau (hTau40, 2N4R, 441 amino acids) of pro-aggregant hTau40/ΔK280 and anti-aggregant hTau40/ΔK280/2P mutants expressed in inducible transgenic mice. The hexapeptide motifs, which show a high tendency to form β-structures (PHF6*, PHF6) are located inside the repeat domain (R1-R4).

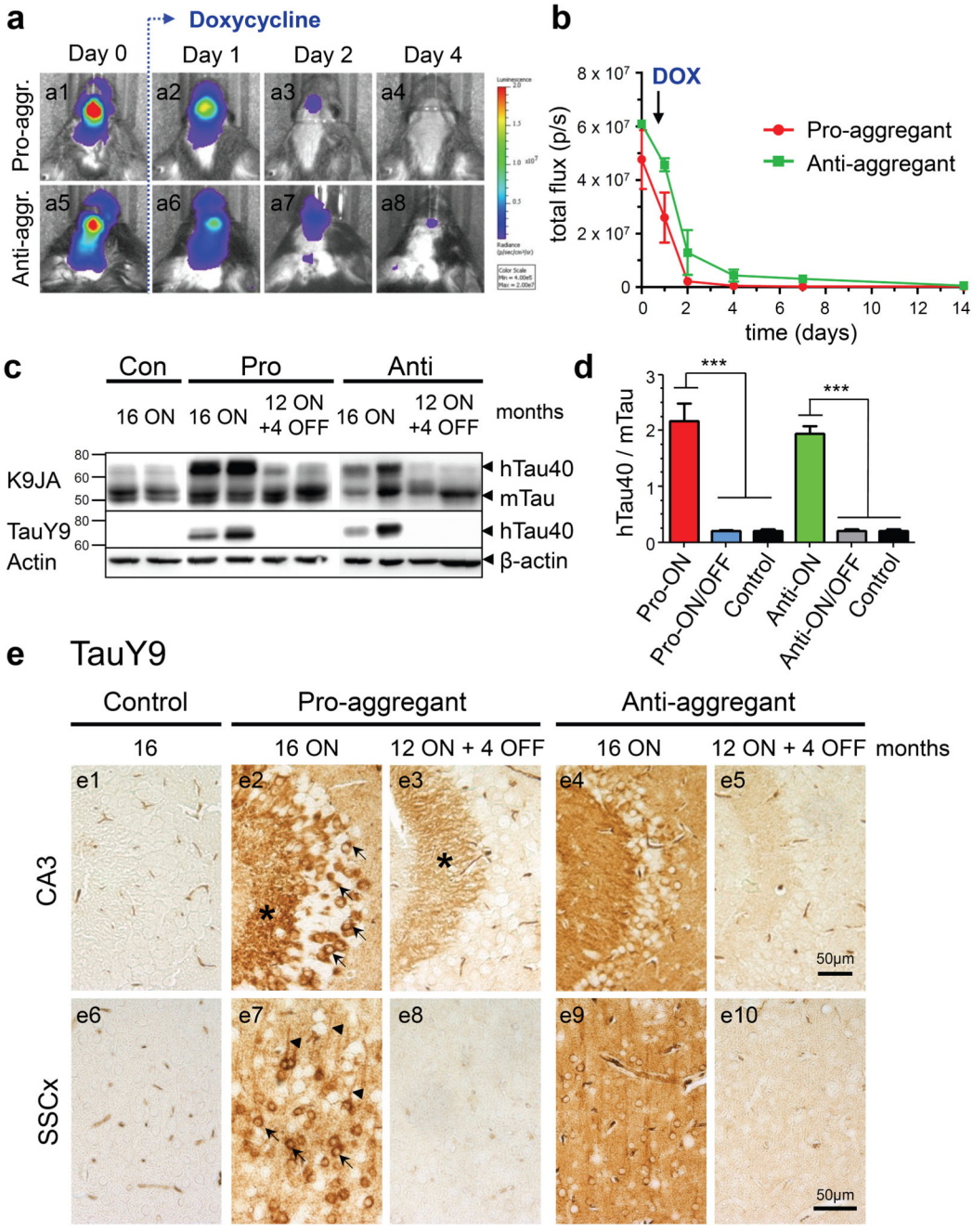

Fig. 2. Characterization of human full-length Tau (hTau40) expression in pro- and anti-aggregant transgenic mice

(a) In vivo bioluminescence imaging (BLI) of luciferase activity. After addition of doxycycline (DOX, 200mg/kg) in food pellets, the transgene expression is down regulated within 4 days in pro-aggregant (a1-a4) and anti-aggregant mice (a5-a8). (b) Quantification of luciferase activity by *in vivo* BLI displayed in photons/s (p/s) after addition of DOX (mean ± SEM, n = 5 mice per group). (c) Representative expression of hTau40 (Mr ~67kDa) and endogenous mouse Tau (mTau, Mr ~45-55kDa) in pro- and anti-aggregant mice. Four months after switch-OFF, a loss of hTau40 is detected by the pan-Tau antibody K9JA and the

Europe PMC Funders Author Manuscripts

Europe PMC Funders Author Manuscripts

human Tau specific antibody TauY9, β-actin serves as loading control. (d) Quantification of (c). Bars indicate the protein ratio of hTau40:mTau (mean + SEM). Pro-ON (n = 12) and anti-ON mice (n = 12) show a ~2-fold overexpression of hTau40 over mTau as compared to pro-ON/OFF (n = 10), anti-ON/OFF (n = 10) and controls (n = 8). ***p<0.0001, one-way ANOVA with post-hoc Bonferroni´s multiple comparison test. (e) Distribution of hTau40 (antibody TauY9) in neurons of the CA3 region (e1-e5) of the hippocampus and somatosensory cortex (SSCx, e6-e10) in control, pro-ON, anti-ON, pro-ON/OFF and anti-ON/OFF mice. Note a mosaic like expression and localization of hTau40 to the cell somata (arrows), *stratum lucidum* (star) and apical dendrites (arrowheads) in pro-ON (e2, e7), whereas anti-ON shows a more diffuse distribution of hTau40 (e4, e9). After switch-OFF, staining intensities in pro-ON/OFF (e3, e8) and anti-ON/OFF (e5, e10) are clearly diminished. Scale bar 50μm.

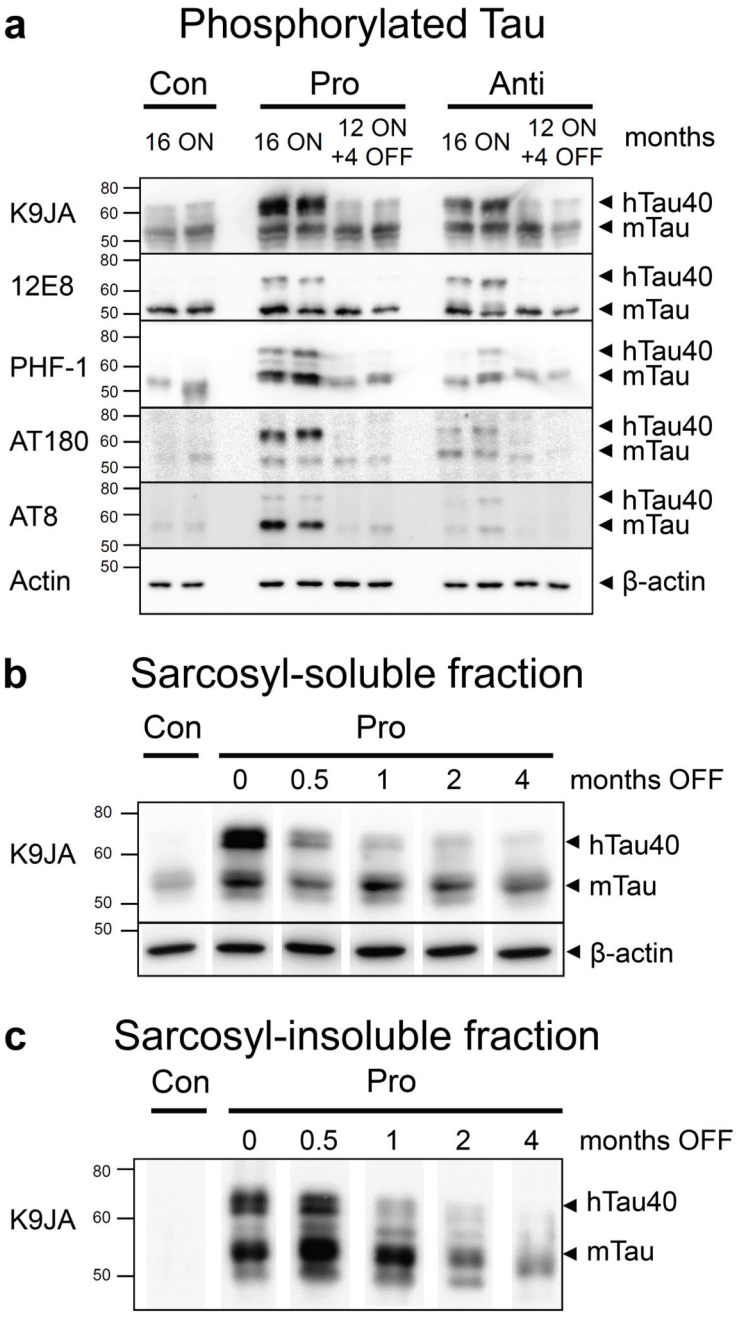

Fig. 3. Tau phosphorylation and aggregation in mice with expression of pro- or anti-aggregant hTau40 and after switch-OFF

(a) Phosphorylated Tau species in hippocampus homogenates of pro-ON and anti-ON (16 months ON) compared to pro-ON/OFF, anti-ON/OFF (12 months ON + 4 months OFF) and controls (16 months). The most prominent phosphorylation of both hTau40 and mTau is detected in pro-ON mice using antibodies against phospho-Tau epitopes 12E8 (KXGS motifs inside the Tau repeat domain, pSer262/pSer356), PHF-1 (pSer396/pSer404), AT180 (pThr231/pSer235) and AT8 (pSer202/pThr205). Anti-ON mice show reduced Tau phosphorylation at epitopes PHF-1, AT180 and AT8 but comparable levels of 12E8

phosphorylated Tau relative to pro-ON. In pro-ON/OFF and anti-ON/OFF mice phosphorylated mTau in the range of control levels is still present. The pan-Tau antibody K9JA indicates expression of human Tau in pro-ON and anti-ON mice, β-actin serves as loading control. (b, c) Sarcosyl extraction of Tau in pro-aggregant (pro) mice with 12 months of gene expression and subsequent switch-OFF for 0.5, 1, 2 and 4 months. (a) Sarcosyl-soluble fraction. Pan-Tau staining with antibody K9JA shows a decrease and finally disappearance of soluble hTau40 over time, whereas endogenous mTau levels remain unaffected. β-actin serves as loading control. (b) Sarcosyl-insoluble fraction. At 12 months, pro-aggregant ON mice show insoluble hTau40 and mTau. Insoluble hTau40 vanishes within 0.5-1 months OFF, whereas insoluble mTau persists over a time period of 4 months OFF but tends to decrease gradually. Control (con) mice do not accumulate insoluble Tau.

Europe PMC Funders Author Manuscripts

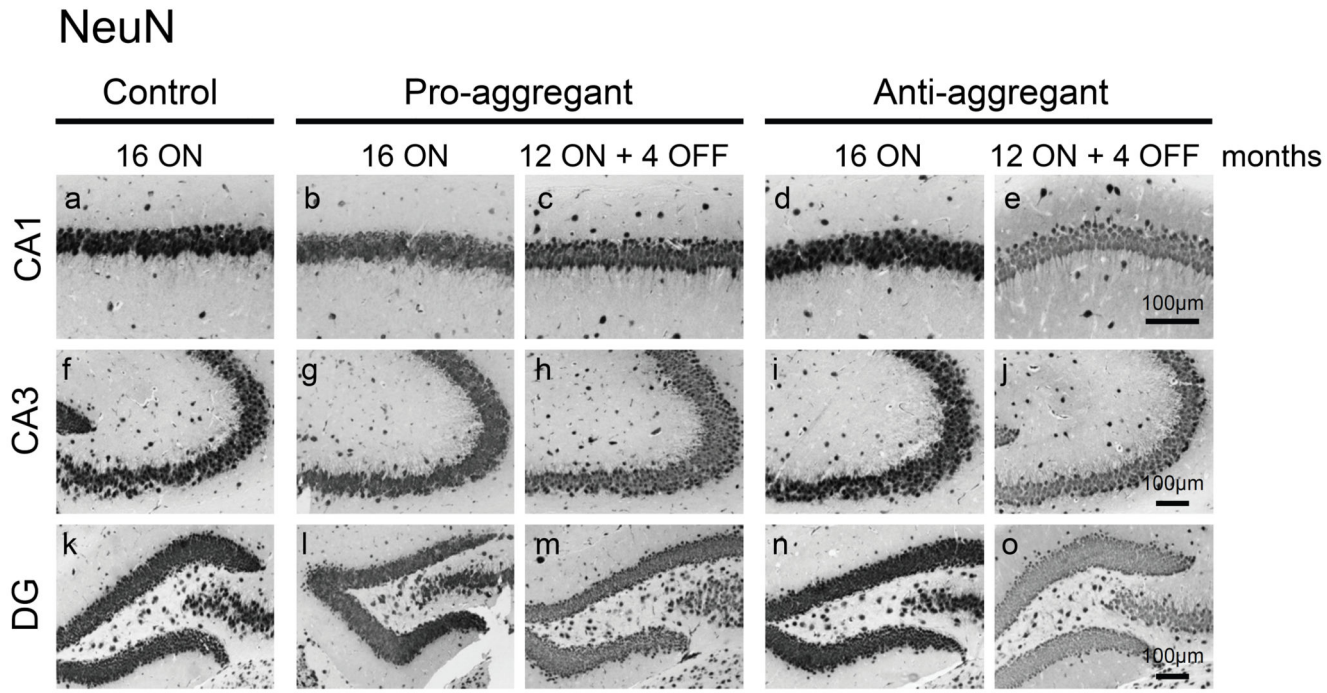

Fig. 4. No neuronal loss upon expression of pro- or anti-aggregant hTau40

NeuN staining depicts no neuronal loss in CA1 (a-e) and CA3 (f-j) regions of the hippocampus or in dentate gyrus (DG, k-o) despite constant expression of pro- and anti-aggregant hTau40 for 16 months. Scale bars: 100µm.

Europe PMC Funders Author Manuscripts

Europe PMC Funders Author Manuscripts

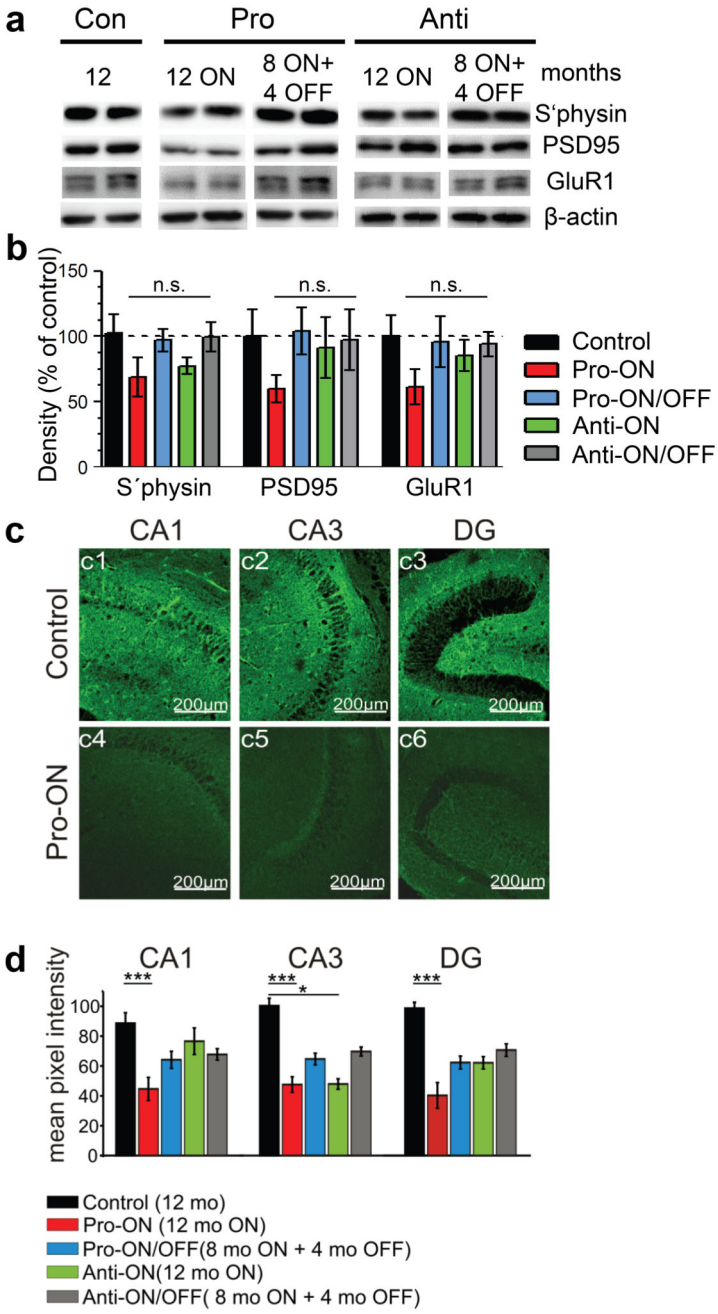

Fig. 5. Expression of pro-aggregant hTau40 results in depletion of synaptic protein levels in the hippocampus, which are restored after switching-OFF the expression of mutant Tau

(a) Representative levels of synaptic proteins synaptophysin (s`physin), postsynaptic density 95 (PSD95) and glutamate receptor 1 (GluR1) in control mice (12 months) compared to pro-ON (12 months ON), pro-ON/OFF (8 months ON + 4 months OFF), anti-ON (12 months ON) and anti-ON/OFF (8 months ON + 4 months OFF). β-actin serves as loading control. (b) Quantification of (a), pro-ON mice show a constant decrease of S´physin, PSD95 and GluR1 levels to ~60% compared to controls. Pro-ON/OFF mice exhibit a full recovery of synaptic protein levels. In anti-ON mice a minor decrease of s`physin to ~77% is detected,

whereas PSD95 and GluR1 levels remain unaffected. Synaptic proteins in anti-ON/OFF mice are comparable to controls. Synaptic protein levels were normalized to β-actin. Bars represent mean ± SEM; (n = 4-5); (n.s.) not significant; s`physin, p = 0.248; PSD95, p = 0.562; GluR1, p = 0.501; one-way ANOVA with post-hoc Dunnett´s multiple comparison test, each column vs. control. (c) Example photomicrographs of synaptophysin immunoreactivity (green) in the hippocampal CA1 and CA3 region and in dentate gyrus (DG). Controls (12 months, c1-c3) are compared to pro-ON mice (12 months ON, c4-c6). Scale bar: 200μm. (d) Mean pixel intensities of s`physin immunoreactivity in horizontal hippocampal slices. Pro-ON and anti-ON (12 months ON), pro-ON/OFF and anti-ON/OFF (8 months ON + 4 months OFF) slices are compared to controls (12 months). S`physin immunoreactivity in pro-ON is significantly decreased in area CA1, CA3 and DG, anti-ON is significantly decreased in area CA3 whereas a partial recovery is observed in pro-ON/OFF and anti-ON/OFF. Bars represent mean ± SEM.*p < 0.01, ***p < 0.001, two-tailed Student´s t-test, n = 3.

Europe PMC Funders Author Manuscripts

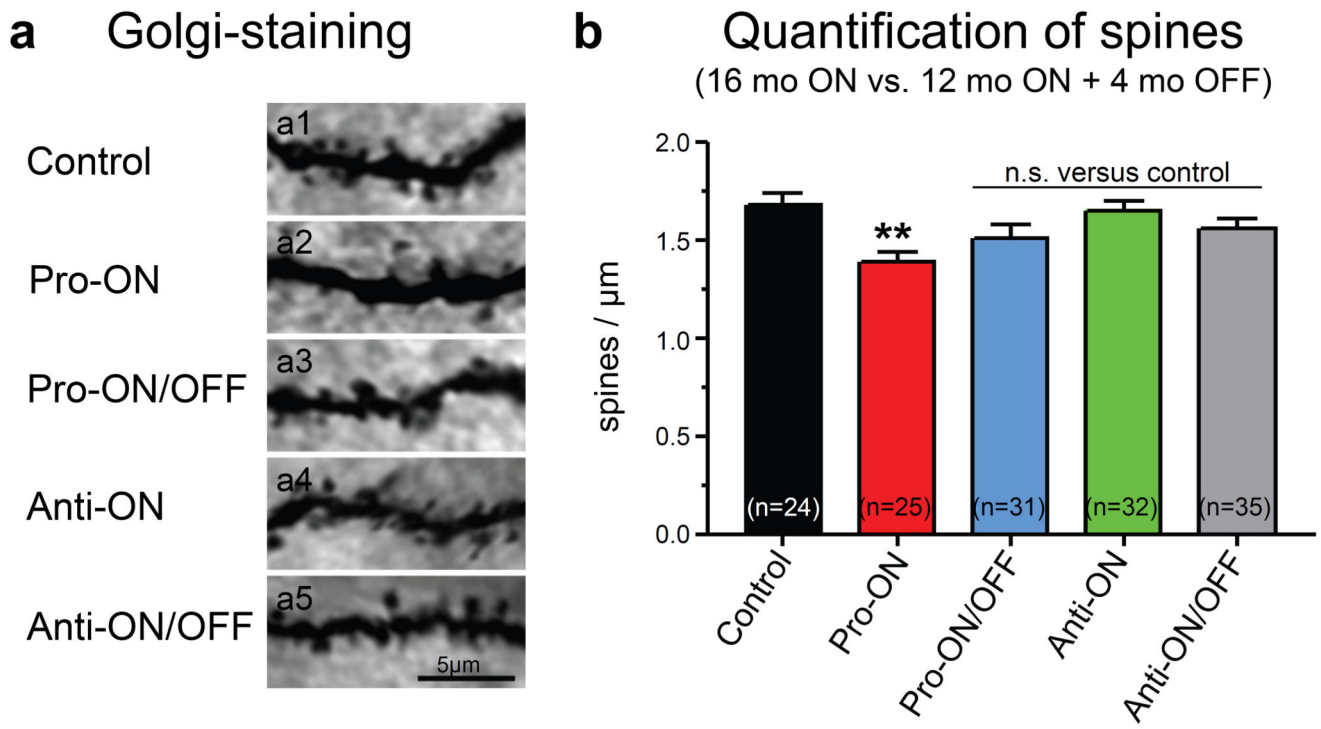

Fig. 6. Dendritic spine densities analyzed by Golgi-staining of neurons

(a) Representative images of apical dendrites of CA1 hippocampal neurons of pro- and anti-aggregant mice compared to control. Scale bar: 5µm. (b) Quantification of (a), a significant reduction of dendritic spines is detected in pro-ON mice (16 months ON, n = 25) as compared to control (16 months, n = 24). Notably, spine densities partly recover in pro-ON/OFF (12 months ON + 4 months OFF, n = 31) mice. No significant change of spine densities is detected for anti-ON (16 months ON, n = 32) and anti-ON/OFF (12 months ON + 4 months OFF, n = 35). N indicates the number of analyzed dendrites. **p = 0.0054, (n.s.) not significant, one-way ANOVA with post-hoc Dunnett´s multiple comparison test, each column vs. control.

Europe PMC Funders Author Manuscripts

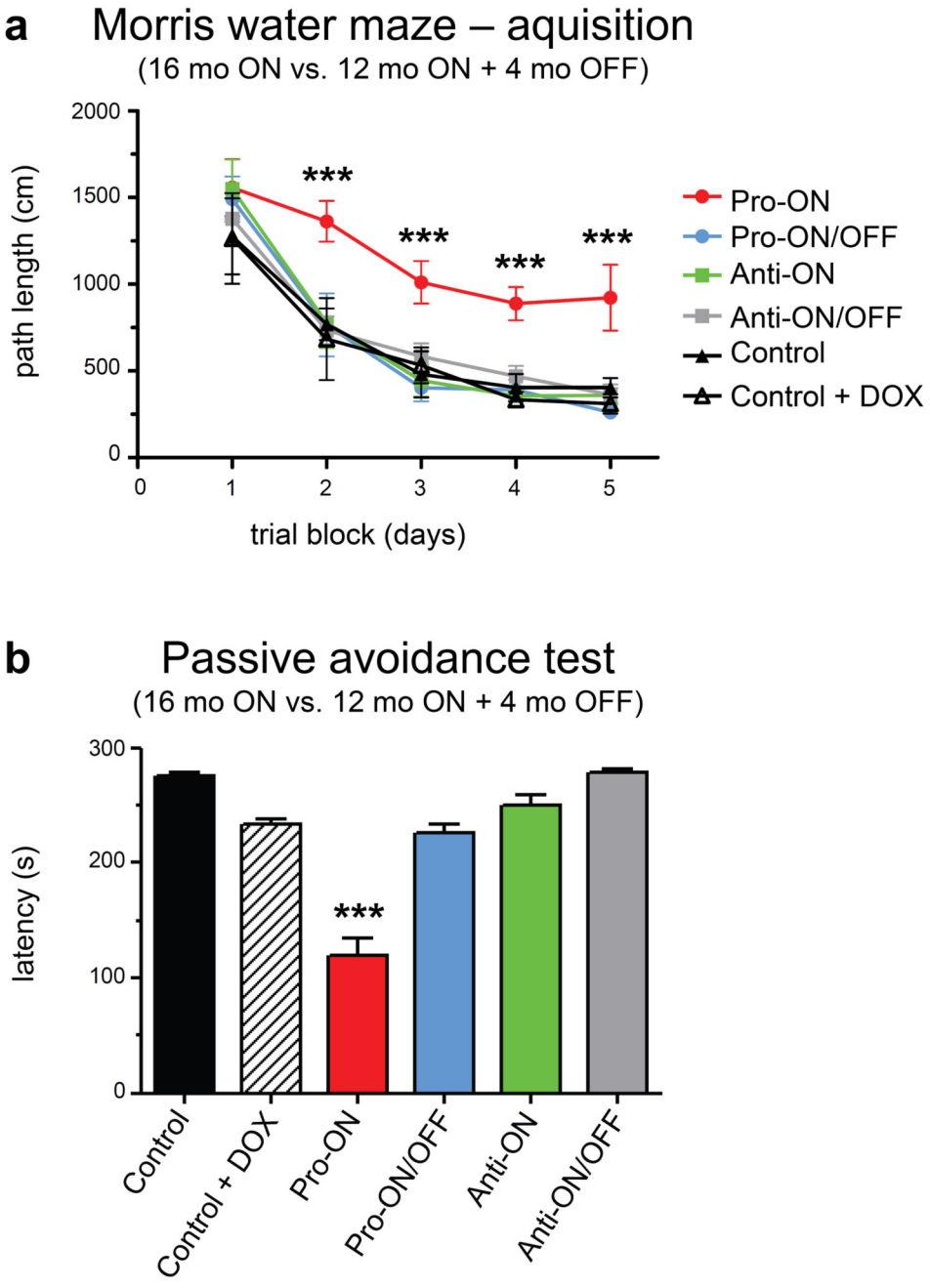

Fig. 7. Cognitive dysfunction of transgenic mice expressing pro-aggregant hTau40 (pro-ON) in Morris water maze (MWM) and a passive avoidance (PA) paradigm

(a) In MWM acquisition only pro-ON mice (16 months ON, n = 6) show spatial learning and memory impairments and fail to learn the position of the hidden platform as indicated by path length, whereas pro-ON/OFF (12 months ON + 4 months OFF, n = 7), anti-ON (16 months ON, n = 7) and anti-ON/OFF mice (12 months ON + 4 months OFF, n = 7) perform similar to controls (n = 7). Note that doxycycline does not influence the learning performance of control mice (n = 5). Data shows mean path length ± SEM. ***$p < 0.001$ [$F(5,136) = 11.02$], two-way repeated ANOVA (one factor repetition) followed by all

pairwise multiple comparison procedures (Fisher LSD method). (b) Pro-ON mice demonstrate disrupted contextual learning and memory as they re-entered the dark compartment in a PA paradigm significantly faster in comparison to pro-ON/OFF, anti-ON, anti-ON/OFF and controls. Bars represent mean latencies ± SEM during the retention trial of a PA task. Pro-ON versus all other groups, ***$p < 0.001$ [$F(5,34) = 46.89$], one way ANOVA followed by all pairwise multiple comparison procedures (Fisher LSD method).

Europe PMC Funders Author Manuscripts

Europe PMC Funders Author Manuscripts

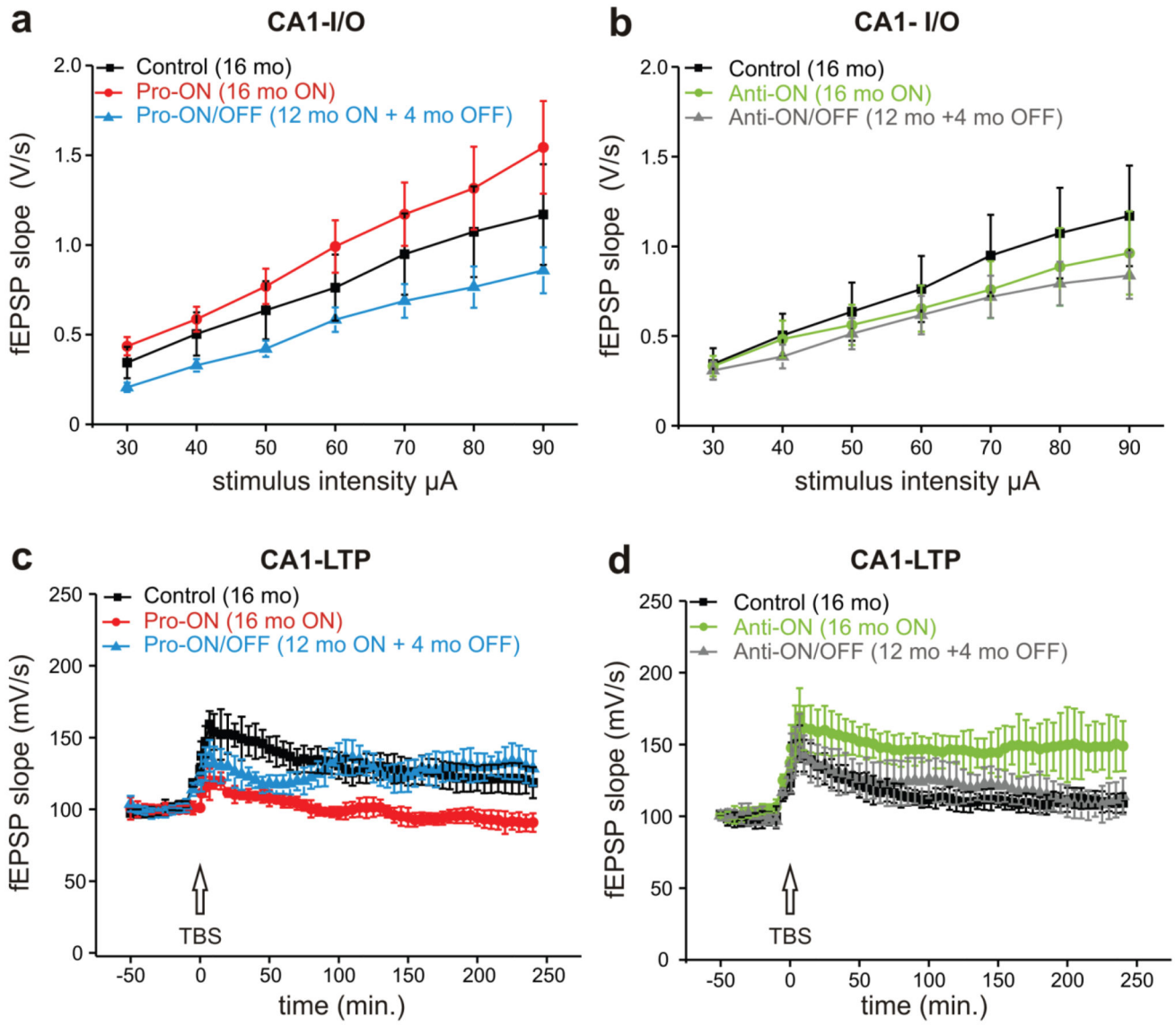

Fig. 8. Dysfunction of the Schaffer collateral pathway in pro-aggregant hTau40 mice

(a, b) CA1 input-output curves of basal synaptic transmission of pro-ON (16 months ON, n = 7), pro-ON/OFF (12 months ON + 4 months OFF, n = 13), anti-ON (16 months ON, n = 7), anti-ON/OFF (12 months ON + 4 months OFF, n = 10) and controls (16 months, n = 10). No differences in basal synaptic transmission are observed between groups in presence or absence of doxycycline. (c) Post tetanic potentiation (PTP) in the first minutes after theta burst stimulation (TBS) is impaired in pro-ON and pro-ON/OFF mice. Long term plasticity (LTP) induced by TBS is significantly attenuated in pro-ON mice ($F = 7.54$, $p < 0.0001$, repeated measure ANOVA), whereas pro-ON/OFF mice show LTP recovery to control level. (d) CA1 LTP in anti-ON mice is significantly enhanced ($F = 18.16$, $p < 0.01$), whereas anti-ON/OFF LTP levels are comparable to control.

Europe PMC Funders Author Manuscripts

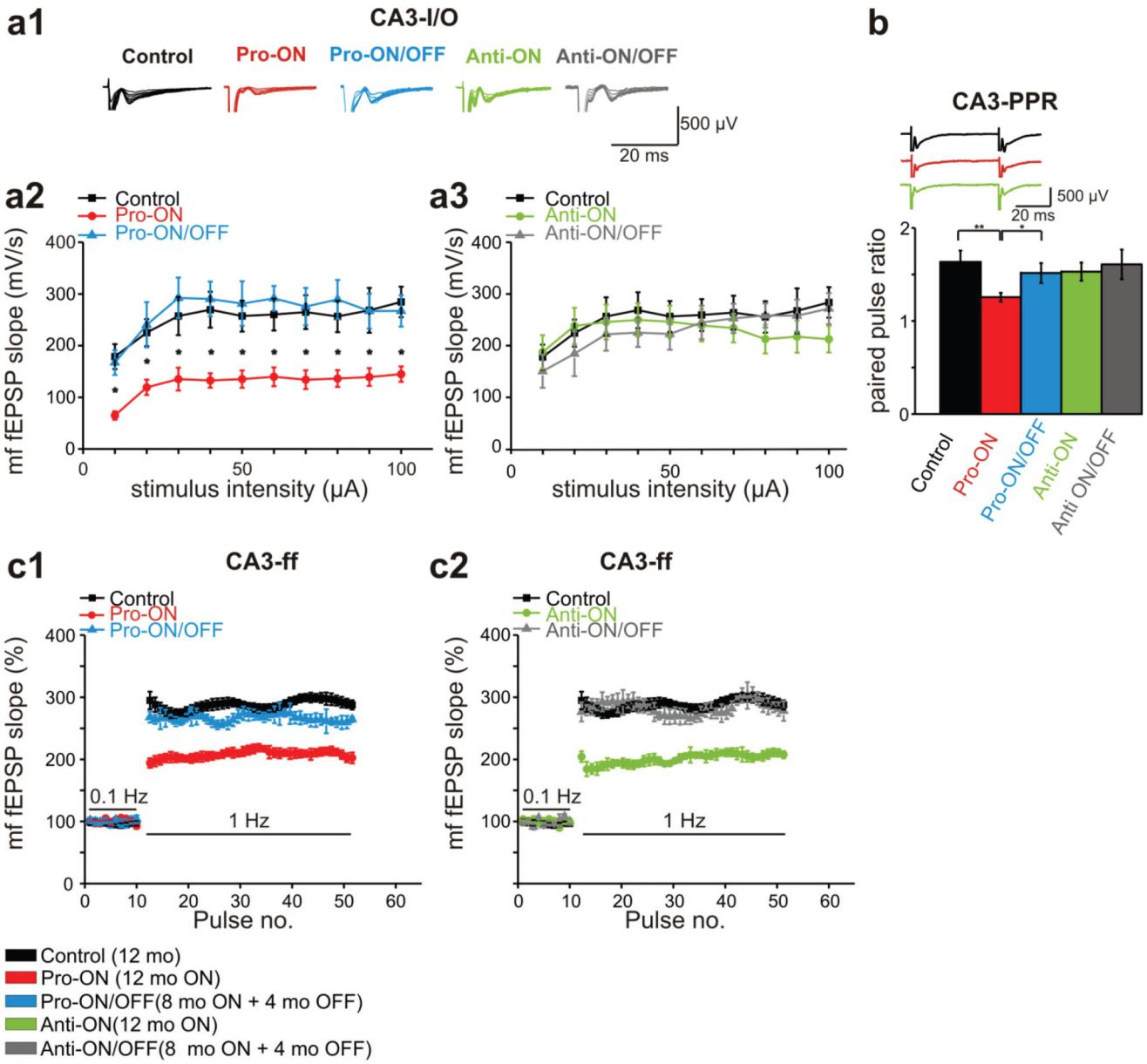

Fig. 9. Mossy fiber dysfunction of basal transmission and short-term plasticity in mice expressing pro-aggregant or anti-aggregant hTau40

(a) Field excitatory postsynaptic potentials (fEPSP) evoked by stimulation of the mossy fiber (mf)-CA3 synapse in the hippocampus of controls (12 months), pro- and anti-ON (12 months ON), pro- and anti-ON/OFF (8 months ON + 4 months OFF) mice. (a1) Representative traces of input-output (I/O) recordings. (a2, a3) I/O curves of mf-fEPSP slopes. Synaptic responses in pro-ON mice are significantly decreased relative to controls ($F = 34.497$, $p = 0.00011$, repeated-measures ANOVA; a2), whereas there is no difference between anti-ON animals and controls ($F = 0.911$, $p = 0.362$; a3). (b) Paired pulse ratio (PPR) at 50ms inter stimulus interval (ISI) is significantly decreased in pro-ON mice compared to controls, pro-ON/OFF, anti-ON and anti-ON/OFF mice. Bars represent mean ±

SEM, *p < 0.01; **p < 0.001, Student´s t-test. (c) Frequency facilitation (ff) is impaired in pro-ON mice compared to controls (F = 22.874, p = 0.00017, repeated-measures ANOVA, c1), anti-ON mice display diminished ff in comparison to anti-ON/OFF and controls (F = 25.795, p = 0.00017, c2). Potentiation of mf-fEPSP slopes at 1Hz is normalized to baseline values stimulated at 0.1Hz. Data represents mean ± SEM.

Europe PMC Funders Author Manuscripts

Europe PMC Funders Author Manuscripts

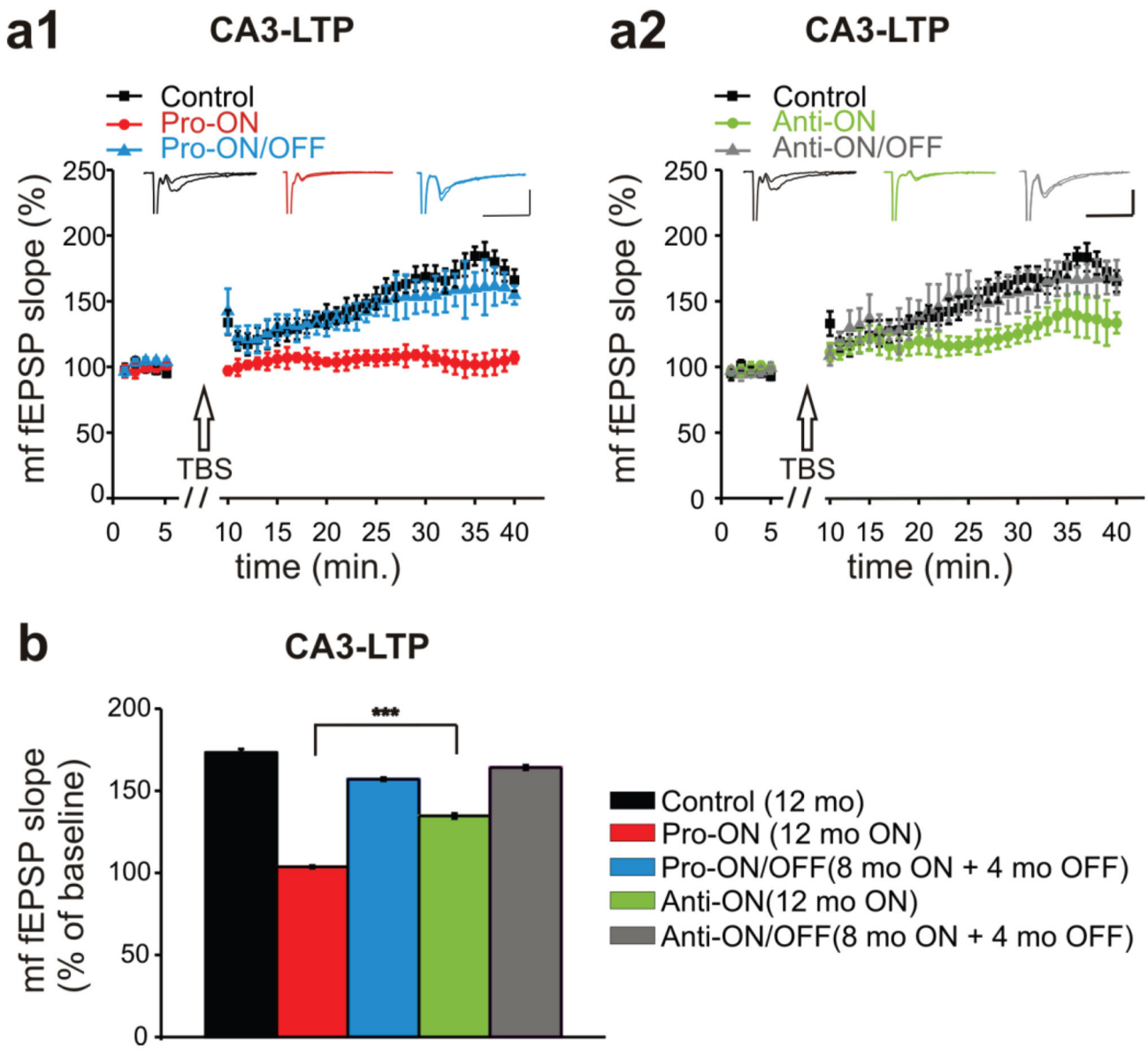

Fig. 10. Mossy fiber long term potentiation (mf-LTP) is attenuated in mice expressing pro-aggregant hTau40

(a) The mf-LTP of pro-ON mice (12 months ON) is significantly diminished relative to controls (12 months) and pro-ON/OFF (8 months ON + 4 months OFF) ($F = 38.301$, $p = 0.0007$, repeated-measures ANOVA, a1). Anti-ON mice (12 months ON) display a reduced mf-LTP in the last 10min of recording compared to controls (12 months) and anti-ON/OFF (8 months ON + 4 months OFF) ($F = 7.0694$, $p = 0.01870$, repeated-measures ANOVA, a2). Scale bars: 500μV and 20ms. (b) The attenuation of potentiation in pro-ON mice was significantly stronger than in anti-ON animals. Bars represent mean ± SEM, ***$p < 0.0001$, Student´s t-test.

Europe PMC Funders Author Manuscripts

Table 1

Neuromotor parameters

	Control		Pro		Anti	
	- DOX	+ DOX	ON	ON/OFF	ON	ON/OFF
Grip strength (mN)	773	779	773	776	780	784
Rotarod (s on rod)	175	200	168	185	204	194
Activity (# crossings)	10667	8838	16130	11211	9078	11256

Pro: pro-aggregant; Anti: anti-aggregant; DOX: doxycycline; ON: 16 months of gene expression; ON/OFF: 12 months ON + 4 months switched-OFF; mN: millinewton; s: seconds; #: number of crossings.

Europe PMC Funders Author Manuscripts

Table 2

CA1 Schaffer collateral plasticity

CA1	basal synaptic transmission		short-term plasticity				long-term plasticity	
	I/O		PPR		PTP		LTP	
Pro-ON	-	n = 13	-	n = 13	↓	158 ± 12%, n = 8	↓	92 ± 6%, n = 8 p < 0.0001
Pro-ON/OFF	-	n = 7	-	n = 8	↓	158 ± 13%, n = 13	-	130 ± 13%, n = 10
Anti-ON	-	n = 10	-	n = 10	↑	198 ± 16%, n = 6	↑	149 ± 18%, n = 6
Anti-ON/OFF	-	n = 7	-	n = 10	↑	198 ± 21%, n = 10	-	114 ± 13%, n = 10
Control	-	n = 10	-	n = 9	-	180 ± 19%, n = 9	-	121 ± 13%, n = 10

Pro-ON: pro-aggregant 16 months ON; Pro-ON/OFF: pro-aggregant 12 months ON + 4 months OFF; Anti-ON: anti-aggregant 16 months ON; Anti-ON/OFF: anti-aggregant 12 months ON + 4 months OFF; Control (16 months); I/O: input/output curve; PPR: paired pulse ratio; PTP: post tetanic potentiation; LTP: long term potentiation; ↓: decrease; ↑: increase; -: no change. Data represents mean ± SEM. Statistical comparison of I/O, PTP and LTP by repeated measure ANOVA; comparison of PPR by Student´s t-test.

Europe PMC Funders Author Manuscripts

Table 3

CA3 mossy fiber plasticity

CA3								
	basal synaptic transmission		short-term plasticity				long-term plasticity	
	I/O		PPR		FF		LTP	
Pro-ON	↓	n = 10 p = 0.00011	↓	1.26 ± 0.047 n = 16	↓	207.76 ± 0.88% n = 11, p = 0.00017	↓	103.7 ± 0.85% n = 7, p = 0.0007
Pro-ON/OFF	-	n = 8	↓	1.51 ± 0.11 n = 17, p = 0.03	-	265.77 ± 9.6% n = 8	-	157.11 ± 0.96% n = 10
Anti-ON	-	n = 10	-	1.53 ± 0.097 n = 16, p = 0.66	↓	200.71 ± 1.28% n = 8, p = 0.00017	↓	134.67 ± 1.66% n = 8, p = 0.01870
Anti-ON/OFF	-	n = 6	-	1.608 ± 0.159 n = 11, p = 0.13	-	282.78 ± 1.68% n = 6	-	164.22 ± 1.37% n = 7
Control	-	n = 10	-	1.63 ± 0.12 n = 26, p = 0.006	-	288.02 ± 1.15% n = 8	-	176.25 ± 2.25% n = 8

Pro-ON: pro-aggregant 12 months ON; Pro-ON/OFF: pro-aggregant 8 months ON + 4 months OFF; Anti-ON: anti-aggregant 12 months ON; Anti-ON/OFF: anti-aggregant 8 months ON + 4 months OFF; Control (12 months); I/O: input/output curve; PPR: paired pulse ratio; FF: frequency facilitation; LTP: long term potentiation; ↓: decrease; -: no change. Data represents mean ± SEM. Statistical comparison of I/O, FF and LTP by repeated measures ANOVA; comparison of PPR by Student´s t-test.